A fragment-based drug discovery strategy applied to the identification of NDM-1 β-lactamase inhibitors

Jérémy Caburet, Benjamin Boucherle, Sofiane Bourdillon, Giorgia Simoncelli, Federica Verdirosa, Jean-Denis Docquier, Yohann Moreau, Isabelle Krimm, Serge Crouzy, Marine Peuchmaur

A fragment-based drug discovery strategy applied to the identification of NDM-1 β-lactamase inhibitors

Jérémy Caburet[a,b], Benjamin Boucherle[a], Sofiane Bourdillon[a], Giorgia Simoncelli[c], Federica Verdirosa[c], Jean-Denis Docquier[c,d], Yohann Moreau[b], Isabelle Krimm[e], Serge Crouzy[b†] and Marine Peuchmaur[a]*

a Univ. Grenoble Alpes, CNRS, DPM, 38000 Grenoble, France

b Univ. Grenoble Alpes, CNRS, CEA, LCBM, 38000 Grenoble, France

c Dipartimento di Biotecnologie Mediche, Università degli Studi di Siena, 53100 Siena, Italy

d Laboratoire de Bactériologie Moléculaire, UR-InBioS, Université de Liège, 4000 Liège, Belgium

e Small Molecules for Biological Targets Team, Centre de recherche en cancérologie de Lyon, Centre Léon Bérard, CNRS 5286, INSERM 1052, Université Claude Bernard Lyon 1, Univ Lyon, Lyon, 69373, France

† S. Crouzy, 17/06/1963-06/04/2020, *in memoriam*

*Marine Peuchmaur, Univ. Grenoble Alpes, CNRS, DPM, Bâtiment E Pôle Chimie BP 53, 38000 Grenoble, France; https://orcid.org/0000-0002-8926-1922

Phone: +33 4 76 63 52 95; Email: marine.peuchmaur@univ-grenoble-alpes.fr

Keywords: NDM-1, metallo-β-lactamase, High throughput virtual screening, Fragment-Based Drug Discovery, STD NMR screening

ABSTRACT

Hydrolysis of β-lactam drugs, a major class of antibiotics, by serine or metallo-β-lactamases (SBL or MBL) is one of the main mechanisms for antibiotic resistance. New Delhi Metallo-β-lactamase-1 (NDM-1), an acquired metallo-carbapenemase first reported in 2009, is currently considered one of the most clinically relevant targets for the development of β-lactam-β-lactamase inhibitor combinations active on NDM-producing clinical isolates. Identification of scaffolds that could be further rationally pharmacomodulated to design new and efficient NDM-1 inhibitors is thus urgently needed. Fragment-based drug discovery (FBDD) has become of great interest for the development of new drugs for the past few years and combination of several FBDD strategies, such as virtual and NMR screening, can reduce the drawbacks of each of them independently. Our methodology starting from a high throughput virtual screening on NDM-1 of a large library (more than 700,000 compounds) allowed, after slicing the hit molecules into fragments, to build a targeted library. These hit fragments were included in an in-house untargeted library fragments that was screened by Saturation Transfer Difference (STD) Nuclear Magnetic Resonance (NMR). 37 fragments were finally identified and used to establish a pharmacophore. 10 molecules based on these hit fragments were synthesized to validate our strategy. Indenone **89** that combined two identified fragments shows an inhibitory activity on NDM-1 with a K_i value of 4 µM.

1. Introduction

Fragment-based drug discovery (FBDD) has been developed during the last twenty years as an innovative approach in the field of medicinal chemistry. For instance, it has successfully been applied in the discovery of compounds which are now in clinical phases [1] mainly in the field of antineoplastic drugs. In anti-infective field, an inhibitor of bacterial topoisomerase II has already reached phase 1 [2]. Usually, a library of filtrated compounds (e.g. according to molecular weight) is screened by virtual or biophysical techniques, especially Nuclear Magnetic Resonance (NMR), X-ray cristallography or Surface Plasmon Resonance (SPR), before structure-guided pharmacomodulation of the selected hits. Virtual screening of fragments is often preferred over physical screening in the early stages of active substance identification mainly for economical reason but also because it can cover a larger chemical space and provide higher hit rates. However, *in silico* screening suffers from many drawbacks especially in the way of classifying putative active small fragments, that remain weak binders at this step [3]. Thus, combining several approaches in order to benefit from the advantages of each of them is of strong interest [4]. In particular, more expensive NMR screening that enables the analysis of ligand and protein-ligand interactions with a high sensitivity could favourably be combined with high throughput virtual screening (HTVS) in a second step.

Since their introduction in therapeutics in the middle of the 20th century, antibiotics have greatly improved public health. However, their misuse and overuse led to rise and dissemination of resistant bacteria strains [5]. The β-lactam family, including penicillins, cephalosporins, carbapenems and monobactams, is a major class of antibiotics. The efficacy of carbapenems, used as "last-resort therapies" for the treatment of severe infections, is now challenged by emergence of bacteria producing carbapenemases [6]. Among them, *Pseudomonas aeruginosa, Acinetobacter baumannii* and *Enterobacteriaceae* are considered by World Health Organization to be a major pathogenic threat requiring the development of new therapies [7]. One of the most prevalent mechanisms of resistance to β-lactam is the hydrolysis degradation of the drugs, mediated by β-lactamases (BL). According to the Ambler classification, [8] these enzymes are divided in four groups. While classes A, C and D present a serine in their active site, class B includes metalloenzymes containing one or two zinc ions in the catalytic pocket.

New Delhi Metallo-β-lactamase-1 (NDM-1), a metallo-β-lactamase (MBL) first discovered at the end of 2008, [9] is now considered as the most clinically relevant target for antibiotic resistance due to its worldwide prevalence [10]. While the combination of antibiotics with serine BL inhibitors (e.g. clavulanic acid or sulbactam) has led to successful therapeutic use, clinically approved MBL inhibitors are still expected. Several studies have been dedicated to the conception of NDM-1 inhibitors and more than 500 compounds have been identified to date [11]. The hydrolysis of the antibiotics β-lactam ring, in NDM-1 active site involves two Zn(II) ions. Therefore, most of NDM-1 inhibitors share common properties or structural features such as chelating agents (e.g. 1,4,7-triazacyclononane-1,4,7-triacetic acid (NOTA)), mercapto alpiphatic acids (e.g. D-captopril) or are natural products (e.g. aspergillomarasmine A (AMA)). Recently, cyclic boronates, such as the pan-spectrum inhibitor taniborbactam (in association with cefepime, phase 3 completed in 2022), or the thiazole carboxylate ANT2681, exhibited promising activity against MBLs [12,13], demonstrating that NDM-1 constitutes an achievable therapeutic target. Nevertheless, none of the NDM-1 inhibitors identified so far has yet been approved: the urge to find new effective inhibitors is therefore still very strong.

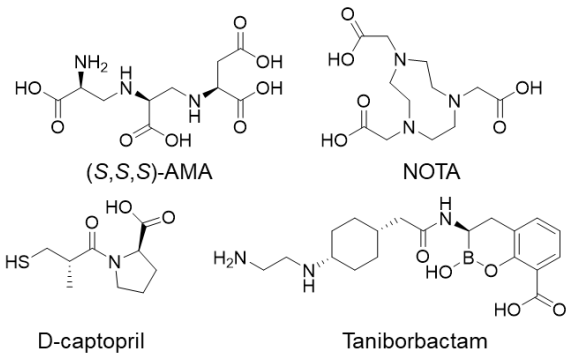

Fig. 1. Structures of known NDM-1 inhibitors

In order to build an efficient library of fragments with significant structural diversity, our FBDD strategy combines HTVS, NMR screening and Density Functional Theory (DFT) calculation to identify fragments able to interact with NDM-1. In practice, well-known and accurate HTVS programs were used on large databank (about 770,000 compounds) to identify virtual hit molecules that were then simplified into fragments of lower molecular weight. Fragments resulting from hit deconstruction were either bought or synthesized to evaluate by NMR their ability to interact as NDM-1 ligands using Saturation-Transfer Difference (STD). At this step, the fragment targeted library (i.e. fragments previously identified through the HTVS process) was broaden with our in-house untargeted fragment library (i.e. some 280 commercially available compounds with a molecular weight lower than 200 $g.mol^{-1}$). Finally, the hit fragments, coming from the targeted or untargeted libraries, could further enter the pharmacomodulation or rationally designed process to fine tune efficient inhibitors of this enzyme.

In this paper, we described our FBDD methodology that led to a proposal of pharmacophore model for future development of MBL inhibitors. *In silico* calculation allowed to predict its interaction with the target, opening the way for further medicinal chemistry development on this scaffold. Finally, the very first preliminary biochemical results illustrate the validity of this multi-technical approach.

2. Results and discussion

2.1. Conception of the targeted fragment library via HTVS

NDM-1, a 270 amino acid protein, belongs to subclass B1 with two Zn^{2+} ions in its active site (Zn_1 and Zn_2). The coordination of Zn_1 involves residues His116, His118 and His196 and shows tetrahedral geometry, completed by the bridging hydroxyde anion. Zn_2 is coordinated following a bipyramidal trigonal geometry by residues Asp220, Cys221 and His263, the bridging hydroxide and a water molecule. The active site of NDM-1 is quite open and delimited by flexible loops, one of them (namely the hydrophobic loop L3) able to somehow close the site entrance or, at the opposite, to shift backward providing more space for bulkier inhibitor/substrate [14].

In order to set up the targeted fragment library, the virtual screening was carried out on the 5ZGE crystal structure of NDM-1 (in complex with hydrolyzed ampicillin) as it displays the best 1.0 Å resolution [15]. After removal of the ligand, the NDM-1 protein structure was prepared (addition of H atoms, determination of the protonation state, multiple occupancies) using the default parameters of the “protein preparation wizard” of the Schrödinger suite of programs [16].

A virtual screening of approximately 770,000 compounds from the French national chemical library (46,000 compounds) [17], the Drugbank (10,000 compounds) [18] and a selection of lead-like molecules of the ZINC15 database (714,000 compounds) [19] was therefore undertaken on this model. Prior to the screening, selected molecules were treated with the LigPrep module of the Schrödinger suite of programs with default parameters [16] to generate different tautomers. Structures with functions considered too reactive were discarded. To narrow the set of compounds taken from the French national chemical library, including large molecules, Lipinsky's rules [20] were applied.

The previously prepared ligand library was subsequently docked using HTVS protocol of Glide module [16]. A receptor grid was created as a cubic cell of 30 Å edges, enclosing the area of co-crystallized ligand that defined the ligand-binding site. Glide SP (Standard Precision) score function was used to select the top 10 % molecules of this virtual screening and the resulting compounds were subjected to another docking step using Glide XP (eXtra Precision) parameters (Fig. 2). Once again, the top 10 % was redocked using the ChemScore function of GOLD software with standard settings [21,22] while the docking area was defined as a sphere of 30 Å of diameter centered on hydroxide ion.

Virtual screening steps	Number of compounds
Combined library	770,000
Glide HTVS	77,000
Glide XP	7,700
GOLD ChemScore	7,700
Consensual best ranked compounds	330
eMolFrag - Datawarrior	100 fragments
Visual inspection	28 fragments
NDM-1 targeted fragment library	

Fig. 2. NDM-1 targeted-fragment library conception

This double docking approach, using programs with different docking methods, has been chosen to allow us to select compounds that are the best ranked by the two (hereafter “consensual” compounds). A visual inspection of the best ranked compounds by both software (Glide XP and GOLD ChemScore, distribution of chemscores and XP docking scores are given in Supporting Information) lead to the selection of 330 molecules from which structures embedded thiol, that have been largely described as MBL inhibitors, were excluded. The resulting compounds were subsequently deconstructed to fragments of lower molecular weight using Datawarrior [23] and eMolFrag [24] generating 40 and 60 fragments respectively. Duplicates and very similar structures were removed from this combined set of fragments, which was also analyzed in light of the structures found in our in-house untargeted fragment library to finally select 16 promising fragments (Fig. 3). These fragments were either synthetized (fragments **13**-**21** and **24**-**27**) using straightforward but not optimized procedures, or bought, when available at a reasonable price (**1**-**12**, **22**-**23** and **28**).

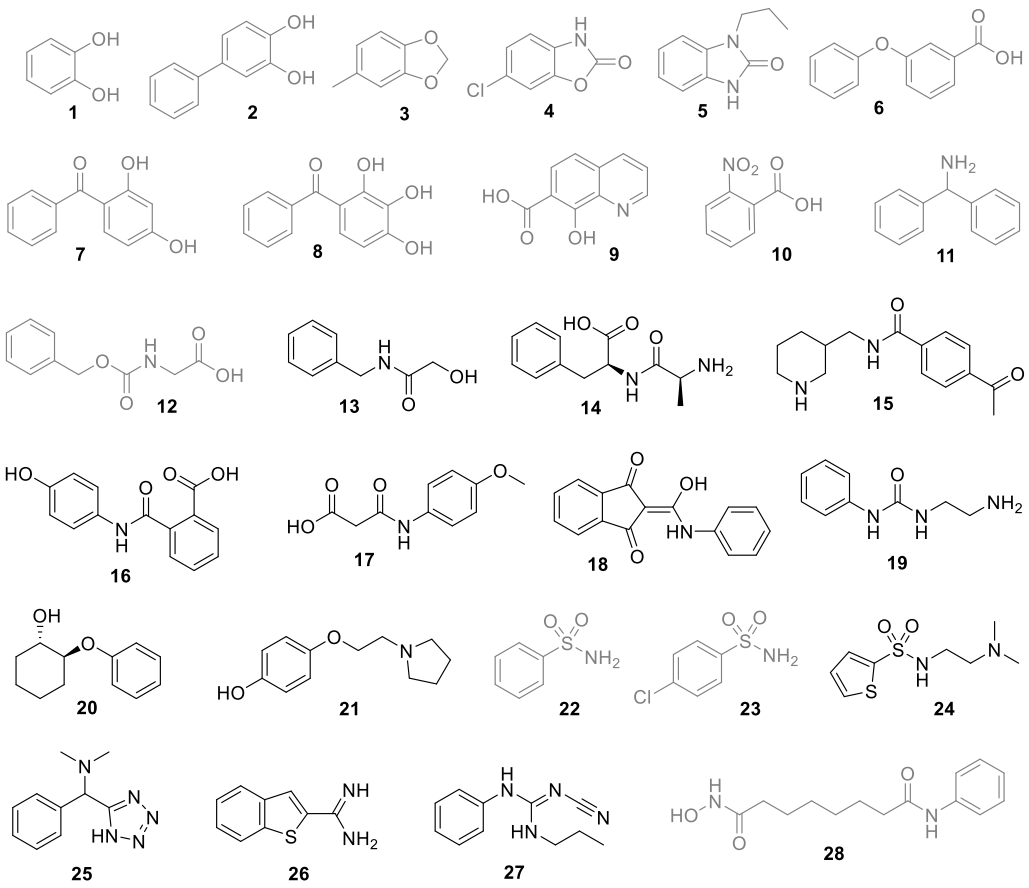

Fig. 3. Structures of putative NDM-1-targeted fragments selected (compounds in black were synthesized whereas those in grey were bought or already available in our in-house fragment library).

2.2. Synthesis of non-commercially available fragments

The synthesis of fragments **13**, **14** and **15** involved a coupling reaction between a carboxylic acid derivative and an aliphatic amine with various coupling agents. Compound **13** was obtained in one step with a relatively low but non optimized yield. Fragments **14** and **15** were obtained as their fluoroacetic salts **14a** (64 %) and **15a** (85 %) after an acidic deprotection of the Boc and/or *t*Bu protecting group respectively (Scheme 1).

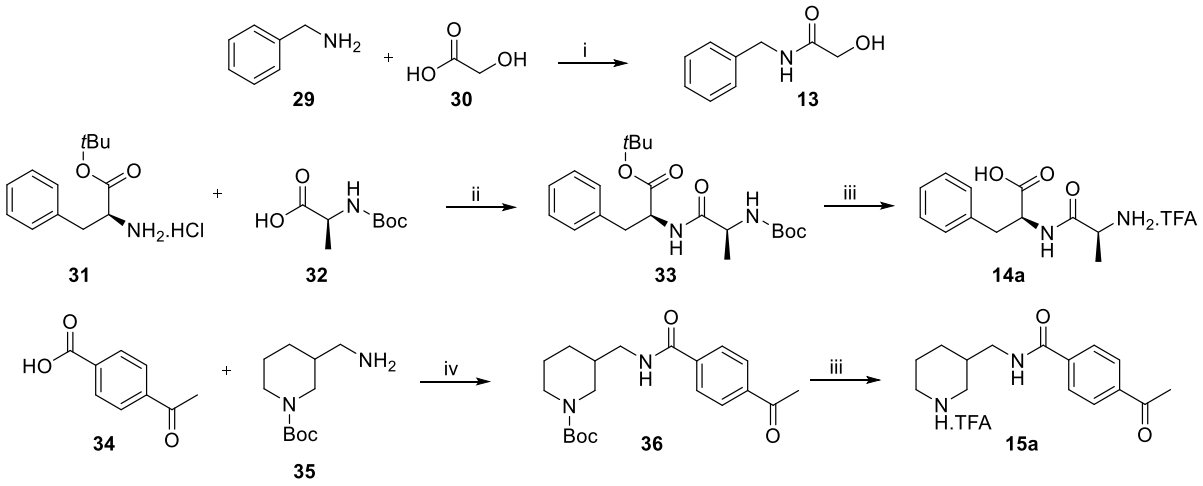

Scheme 1. Synthesis of fragments **13**, **14a** and **15a**. Reagents and conditions: (i) DCC, HOBt, CH_2Cl_2, rt, 28 %; (ii) EDC, HOBt, DMAP (cat), NEt_3, CH_2Cl_2, 0 °C to rt, 64 %; (iii) CH_2Cl_2, TFA (1:1), rt, quant. for **14a** and 89% for **15a**; (iv) TBTU, DIPEA, DMF, rt, 96 %.

Amide bonds of fragments **16** and **17** were respectively formed starting from *p*-aminophenol and phthalic anhydride **38** or *p*-aniside and Meldrum's acid **40** with low yields due to the poor nucleophilicity of aniline derivatives (Scheme 2).

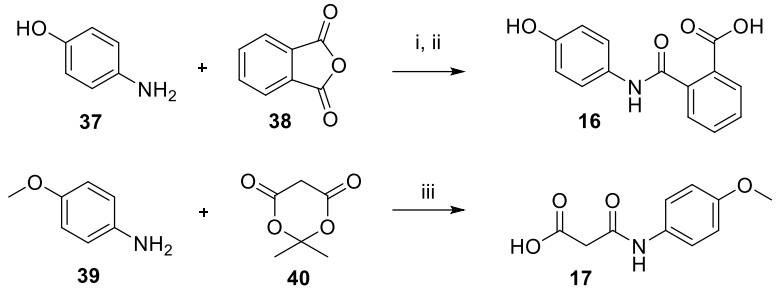

Scheme 2. Synthesis of fragments **16** and **17**. Reagents and conditions: (i) pyridine, CH_2Cl_2; (ii) HCl 1 M, H_2O, rt, 27 %; (iii) H_2O, reflux, 38 %.

Phenylisocyanate was used to synthesize fragments **18**, which can be described as a multi tautomer indenedione, and **19**, an arylurea which was obtained as its trifluoroacetic salt **19a** with 73 % for two steps (Scheme 3) [25].

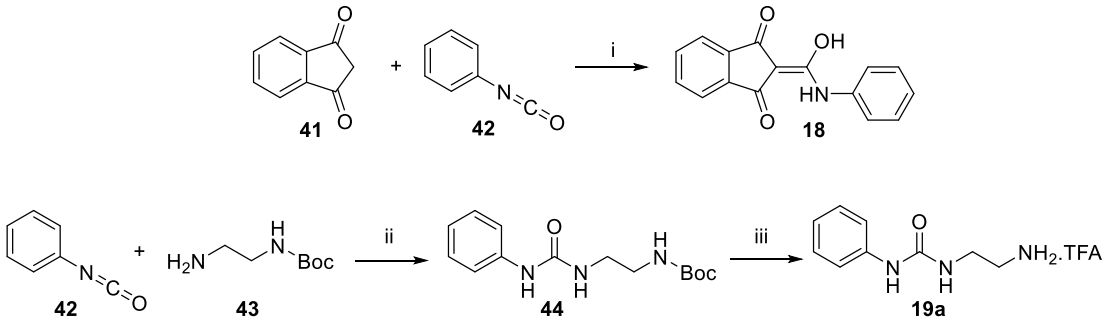

Scheme 3. Synthesis of fragments **18** and **19a**. Reagents and conditions: (i) NEt_3, DMF, –35 °C, 56 %; (ii) CH_2Cl_2, rt, 73 %; (iii) CH_2Cl_2, TFA (1:1), rt, quant.

Two phenoxy derivative fragments **20** and **21** were synthetized using phenolate, through epoxide opening of compound **45** or Williamson reaction on compound **48** followed by hydrogenolysis of benzyl ether protecting group (Scheme 4).

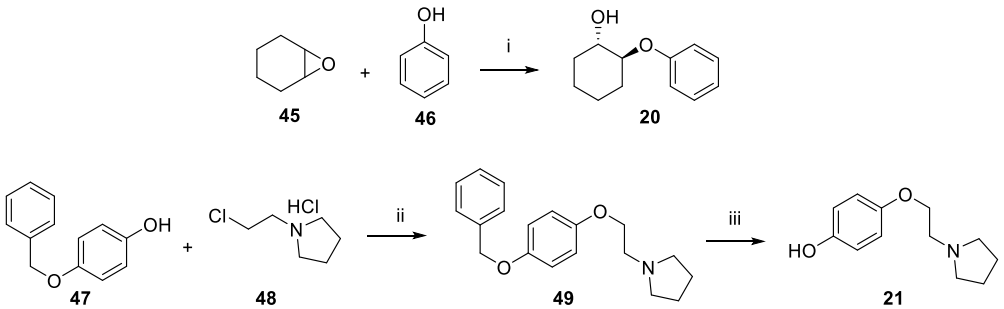

Scheme 4. Synthesis of fragments **8** and **9**. Reagents and conditions: (i) *t*BuOK, *t*BuOH, THF (1:1), reflux, 44 %; (ii) K_2CO_3, Cs_2CO_3, DMF, rt, 36 %; (iii) H_2, 10 % Pd/C, EtOH, rt, 61 %.

Two fragments embedding aliphatic tertiary amines **24** and **25** were synthesized. Sulfonamide formation starting from the corresponding sulfonyl chloride **50** afforded compound **24** with 71 % yield (Scheme 5). Fragment **25** was obtained in two steps by an original methodology developed by Fuentes *et al.* [26].

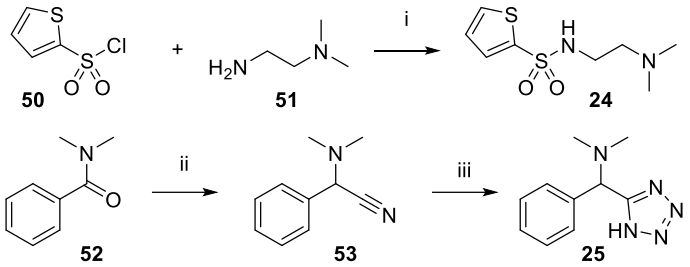

Scheme 5. Synthesis of fragments **24** and **25**. Reagents and conditions: (i) NEt_3, CH_2Cl_2, 0 °C to rt, 71 %; (ii) TMDS, TMSCN, $Ir[(PPh_3)_2ClCO]$ (cat.), toluene, rt, 85 %; (iii) Bu_2SnO, $TMSN_3$, toluene, 70 °C, 41 %.

Fragments **26** and **27** were both obtained in two steps. Compound **26** was obtained as its trifluoroacetic salt **26a** by a nucleophilic aromatic substitution of thiol **55** on 2-fluorobenzaldehyde **54** followed by a cyclisation. The methylic ester conversion of intermediate **56** to amidine lead to fragment **26a** (Scheme 6). Finally, the fragment **27**, displaying an original cyanoguanidine group, was synthesized by two nucleophilic substitutions on dimethylcyanocarbonimidodithioate **58**: the first one involved the aromatic amine **57** and the second one the propylamine.

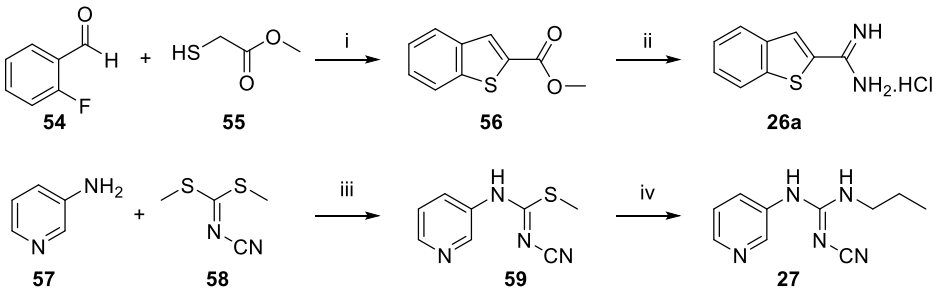

Scheme 6. Synthesis of fragments **26a** and **27**. Reagents and conditions: (i) K_2CO_3, DMF, 80 °C, 56 %; (ii) $AlMe_3$, NH_4Cl, toluene, reflux, 85 %; (iii) NaH (60 % in oil), DMF, 0 °C to rt, 37 %; (iv) propylamine, pyridine, 55 °C, 44 %.

2.3. NMR screening of the targeted and untargeted fragment libraries

A screening of the combined fragment libraries (NDM-1-targeted and non-targeted) was performed on 300 fragments using ^{1}H WaterLOGSY sequence on mixtures of 5 to 10 fragments in presence of NDM-1 protein. An analysis of the STD NMR experiments highlighted interactions between 37 fragments and the targeted protein (Fig. 4). Among them, 13 fragments come from the targeted library (compounds in black), which implies that these compounds were first identified after the virtual

screening and then their possible interaction with NDM-1 was confirmed by NMR analyses. Looking more specifically at these fragments that followed the entire design process, four of them have never been described to interact with any metalloenzyme (**4**, **5**, **18**, **26**). Fragments **9** and **28** are known to interact with metalloenzyme, Influenza endonuclease [27] and HDAC [28] respectively, but they were not studied as MBL inhibitors. However, 8-hydroxyquinoline derivatives have been recently described as NDM-1 inhibitors [29,30]. Fragment **6** was already described as a carbonic anhydrase inhibitor [31] while fragments **3**, **11** and **23** are present in some NDM-1 inhibitors [32–35]. Nevertheless, these fragments are not the central part of the inhibitors described in the literature, i.e. they were neither subjected to pharmacomodulation nor systematically studied as worthwhile substituent (only 1 or 2 examples of each fragment could be found): further work could thus interestingly use fragment linking or merging to introduce more frequently these moieties to obtain larger inhibitors. Fragments **2**, **7** and **8** have never been described as metalloenzyme inhibitors with this complexity, however the smaller 2-hydroxyacetophenone (2-HAP) and catechol fragments are known to interact with the Zn ions of NDM-1 binding site [36]: these two shorter fragments will be subsequently retained for the next part of the study. All together, these results are highly satisfactory since they highlight the relevance of our methodology: known structures have been found again through the process while new and innovative fragments have also been identified.

Concerning the additional untargeted fragment library, the results could significantly broaden the diversity of the final set of relevant fragments that could be used in the design of fine-tuned inhibitors of NDM-1. Nonetheless, it should be noted that some structures are known to be frequent hitters in high-throughput NMR screening: these especially include arylmethanol such as **78** or biaryl derivatives (usually made up of a phenyl and a 5- or 6-membered nitrogen heterocycle such as **68**, **69** or **73**). It is worth mentioning that fragment **80**, the 8-hydroxyquinoline (8-HQ), identified as a fragment hit in the untargeted library is a very close analogue of fragment **9** that originated from the targeted library, and also an isomer of fragment **81** (itself a close analogue to fragment **82**).

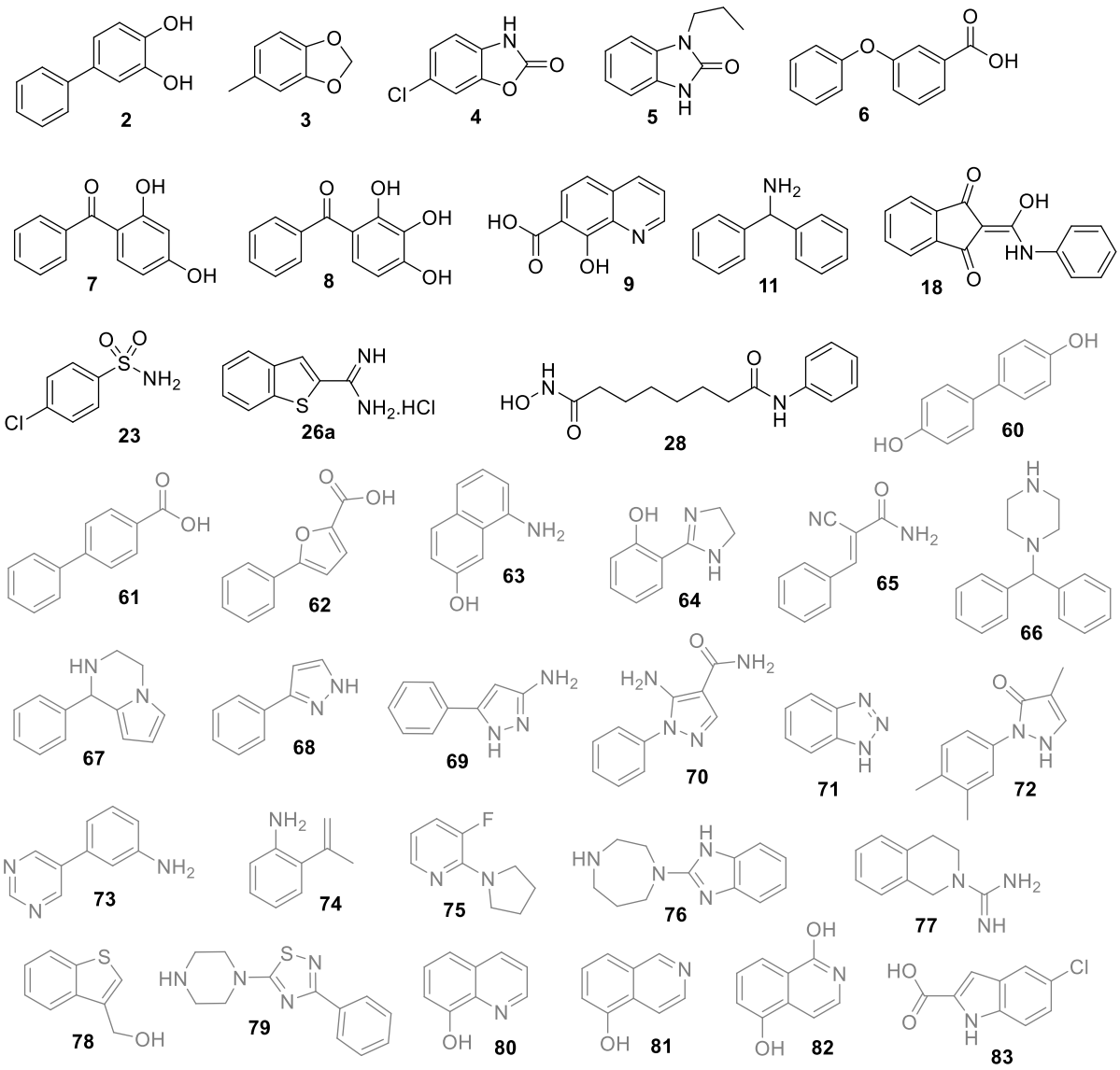

Fig. 4. NDM-1 binding fragments identified through STD NMR experiments (compounds in black originated from the targeted library whereas those in grey come from the non-targeted library).

2.4. Pharmacophore model and Density Functional Theory calculation

The 37 binding fragments shown in Fig. 4 have been used to generate 3D models *via* a pharmacophore analysis using the Phase module of the Schrödinger suite [16]. To do so, a distance tolerance of 1.5 Å, the requirement of 4-5 features were imposed (e.g. hydrogen acceptor/donor) and multiple conformers generated. Three pharmacophore models were thus generated. The best phase score of 0.463 was obtained for the model containing four pharmacophoric features: one hydrogen acceptor, one hydrogen donor (red and blue spheres respectively, the arrows specifying the possible direction of the interaction) and two aromatic rings (orange circles) (Fig. 5).

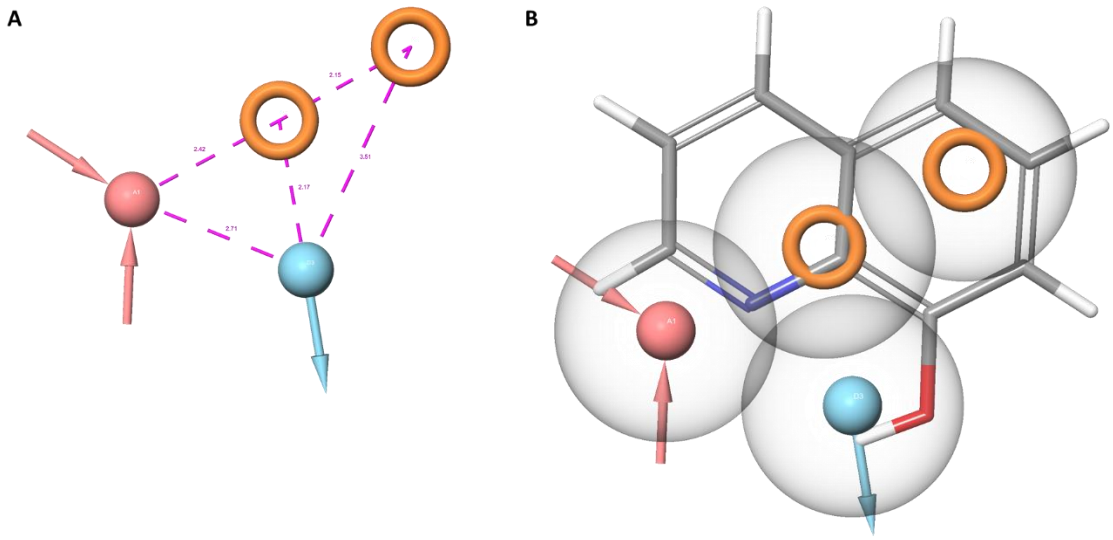

Fig. 5. Generated pharmacophore model. **A.** Distance in Å between pharmacophoric features; **B.** Pharmacophore alignment with the selected fragment **80** (8-HQ) with a spherical position tolerance of 1.5 Å.

Among the 12 fragments fitting to the pharmacophoric description (i.e. fragments **4**, **5**, **9**, **63**, **68**-**72**, **78**, **80** and **82**), the 8-HQ (fragment **80**), that belongs to a well-represented family in the NMR screening, was chosen. Furthermore, 8-HQ was previously identified as pertinent structure to develop MBL inhibitors (even NDM-1 more recently): a deeper study of this interaction with NDM-1 seems appropriate. Actually, because of the phenol being in close proximity to the hydroxide ion (2,61 Å between the hydrogen of the phenol and the oxygen of HO^- based on the results of molecular modelling), a proton exchange that could not be described by classical forcefields could be considered. To gain insight into the interaction between the 8-HQ fragment and the active site of NDM-1, DFT calculations were thus conducted. In the end, this study could help the rational design of new inhibitors indicating for example the best position to modulate and optimize the fragment, in particular by growing or linking strategies. Three systems were therefore studied: active site alone (Zn_2-HO^-, noted S0 in fig. 6), ligand alone and the different complexes of both (noted S1, S2 and S3). In this approach, an approximate binding interaction is determined as the energy of the latter subtracted from energies of site and ligand alone. The "site+ligand" complex is the structure obtained after optimizing the model that originated from docking results on which a proton transfer occurred spontaneously between the acidic phenolic function of 8-HQ and the hydroxide ion of the active site. The phenolate ion is able to bind Zn_2 whereas H_2O remains linked to Zn_1. Furthermore, another interaction between the 8-HQ nitrogen and the residue Lys_{211} appeared in S1. Ultimately, the difference of energy, around –35 kcal/mol, highlights a very favorable interaction. Moreover, the fact that the Zn_1–O_{OH} distance has been little varied between states S0 and S1 whereas the Zn_2–O_{OH} and Zn_1–Zn_2 distances were increased suggests that the interaction between H_2O and Zn_2 is essential for the deprotonation.

During this study, it was noticed that H_2O could be moved between Zn_1 and Zn_2 thus making room for the phenolate to both coordinate with Zn_1 and Zn_2 (S2). Simultaneously, the quinolone nitrogen coordinates Zn_2 (distance of 2.19 Å). The difference between the internal energies of S1 and S2 is very low, approximately –1 kcal/mol, suggesting that these two systems are probably in equilibrium.

Finally, we consider a "site+ligand" complex in which H_2O will be released of the active site (S3). However, the change in the internal energy of the system is then unfavorable (+20 kcal/mol). This

result highlights that the interaction between H_2O and Zn_1 is relatively strong in the active site of NDM-1, which is not the case for an aminopeptidase from *Aeromonas proteolytica*, another dinuclear zinc enzyme. Indeed, this protease was co-crystallized with 8-HQ and the RX crystallography showed that the hydroxide ion is not present in the complex: the phenolate bridges the two Zn ions as in a structure similar to the S3 complex (Fig.6) [37].

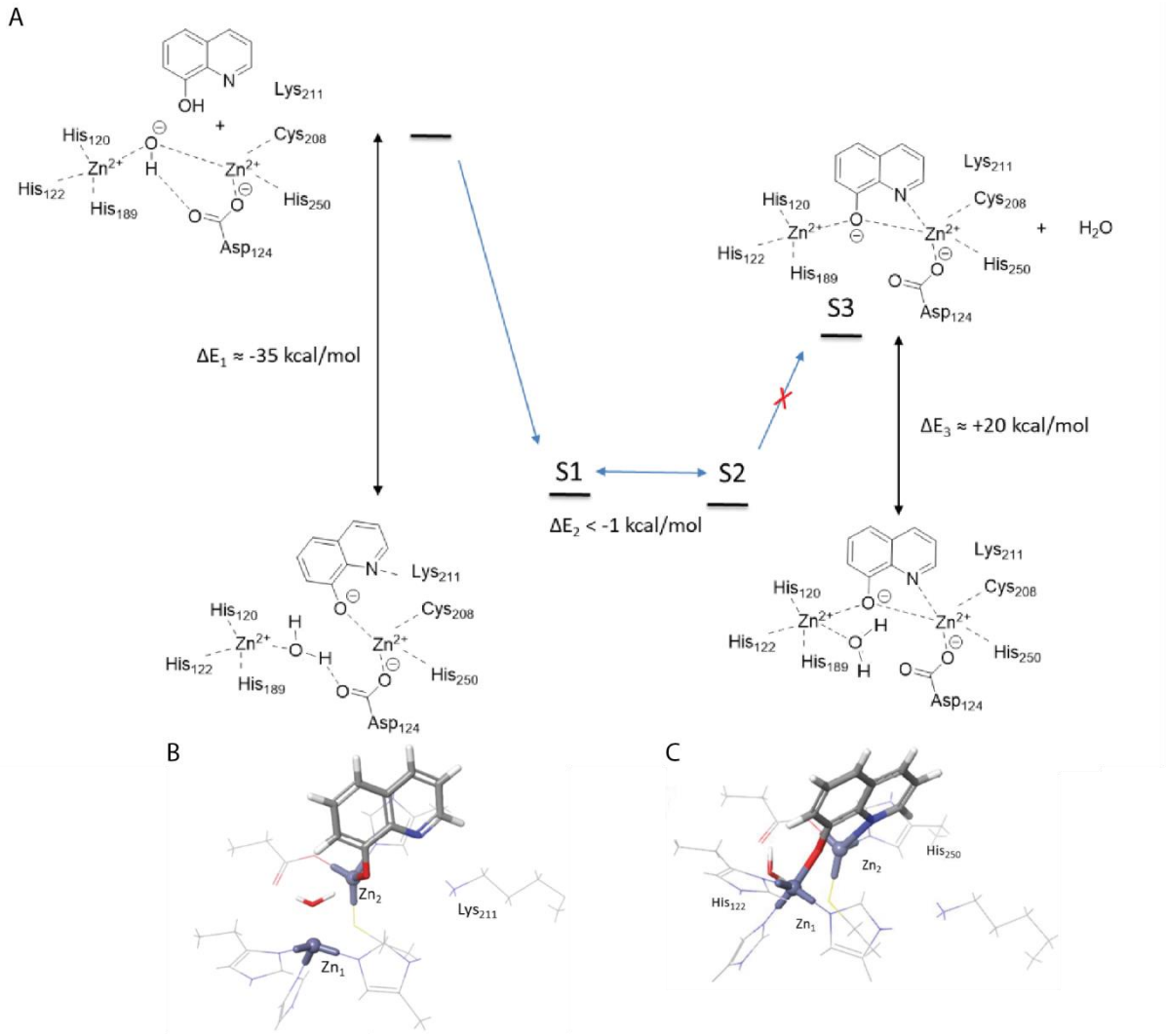

Fig. 6. A. DFT calculation of 8-HQ in the active site of NDM-1; 3D representation of 8-HQ in the active site: **B.** Complex S1; **C.** Complex S2.

The orientation of 8-HQ in the active site of NDM-1 allows the identification of several positions that could be pharmacomodulated in order to design larger molecules with improved affinity and/or selectivity for NDM-1. Indeed, a substitution at positions 2 or 3 would allow interaction with the residues Asp_{212}, Lys_{216}, Ser_{217}, Ser_{251} whereas positions 6 and 7 are properly directed on the residues Gln_{123}, Glu_{152}, Asp_{223}. Positions 4 and 5 are oriented towards the hydrophobic loop L3.

2.5. First biochemical assays to validate the methodology – synthesis of molecules inspired by fragments

With a view to promptly and effectively validate our methodology and the fragments identified as potential ligand of NDM-1, we first screened some flavonoids available in our laboratory (Table 1). The synthesis of these flavonoids was previously described [38,39]. Compounds **84**-**89** were chosen because of their original structure compared to NDM-1 inhibitors flavonoids-based already described and because some of these flavonoids combine at least two fragments of interest (or with a structure close to them). These preliminary results tend to show that, among flavonoids, chalcones (e.g. **84**-**86**) are not a privilege structure to bind NDM-1 compared to aurone (e.g. **87**-**88**) or even more indenone (e.g. **89**) scaffolds. In particular, the indenone **89** which structure linked the 2-HAP and the catechol fragments was identified to strongly inhibit NDM-1. This inhibitor is quite selective of this MBL since its activity on VIM-2 and IMP-1 are much lower (selectivity of compounds inactive or slightly active on NDM-1 was not evaluated). For indenone **89**, the K_i on NDM-1 was determined to be as low as 4.1 ± 0.3 µM. The aurone **87** have a similar biological result profile with a K_i close to 5 µM (4.8 ± 0.5 µM). Consequently, it would be of great interest to pursue this work by leading structure-activity relationship studies on these two families of flavonoids.

In addition, as part of our goal to validate this rational methodology, we decided to synthesize some 8-HQ derivatives in light of the DFT calculation and the fragments identified by NMR and virtual screenings. The fragment **80** was identified as NDM-1 binding fragment through STD NMR experiments but the close fragment **9** was first identified by virtual screening. This fragment belongs to a larger molecule that could be used to guide the first analogues to synthesize. Based on the structure of the hit compounds **95**, first described as an inhibitor of HIV-1 integrase which contains two divalent metal cations in its active site [40], compound **90a** that combines 8-HQ and fragment **3**, and **90b** that includes only one identified fragment were synthesized. Two analogues were also obtained: hydrogenation of the exocyclic double bound of compound **90a** and **90b** gave the corresponding flexible compounds **91a** and **91b** respectively.

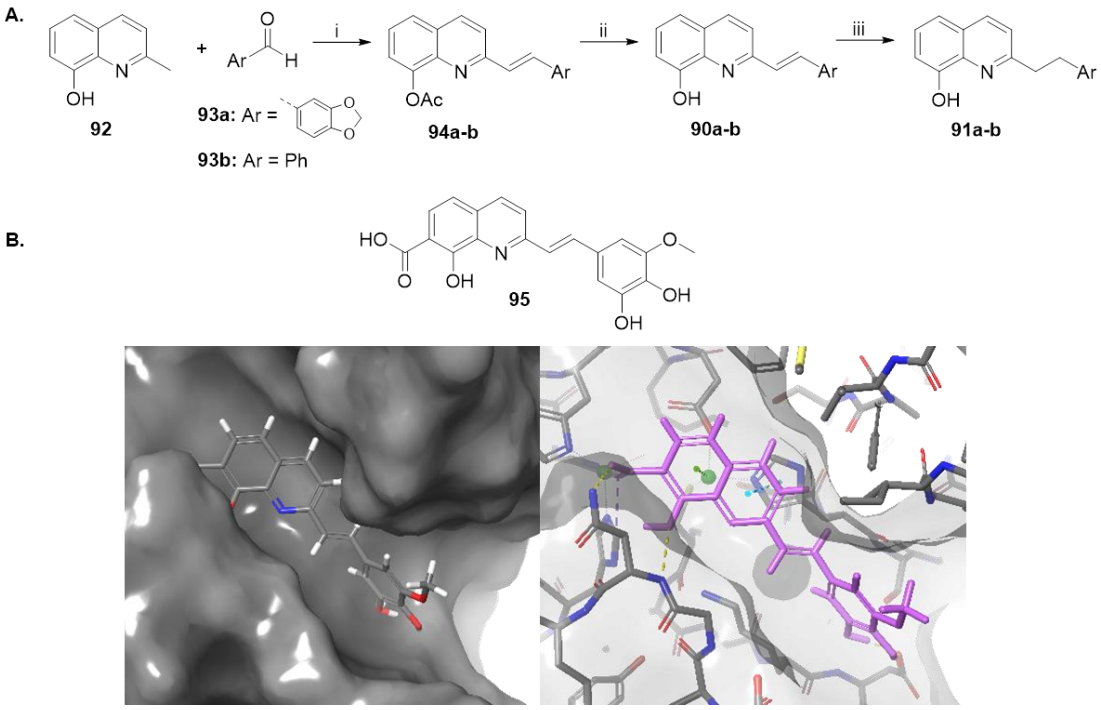

Fig. 7. A. Synthesis of compounds **90-93**. Reagents and conditions: (i) Ac_2O, 130 °C, 14 and 78 % (**94a** and **94b** respectively); (ii) HCl 37 %, EtOH, reflux, 81-87 %; (iii) H_2, Pd/C 10 %, EtOAc, rt, 54-64 %. **B.** Hit

molecule **95** identified through virtual screening on NDM-1 and its docking pose with dotted line representing interactions with the protein (yellow: H bond, purple: aromatic H bond, blue π-π stacking, green π-cation).

Compounds **90a** and **91a**, embedding two fragments of interest, are slightly more active on NDM-1 than the phenyl analogue **91b**. However, the activity of analogue **90b** is similar to those of **90a** and **91a** what mitigating the benefit of the two fragments linking strategy here although a wider study may be required to really conclude. Moreover, these four 8-HQ derivatives also present an inhibitory activity on IMP-1 whereas they are only moderately active on VIM-2 (Table 1).

Table 1. Biochemical evaluation of compounds **84**-**91** on NDM-1 and possibly VIM-2 and IMP-1 (percentage of inhibition at 50 µM).

Entry	Structures	Inhibition (%) at 50 µM		
		NDM-1	VIM-2	IMP-1
1	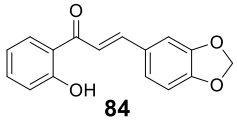 **84**	≤ 20	-	-
2	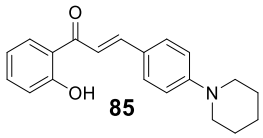 **85**	35 ± 4	-	-
3	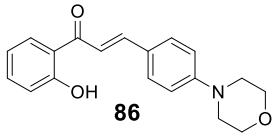 **86**	24 ± 13	-	-
4	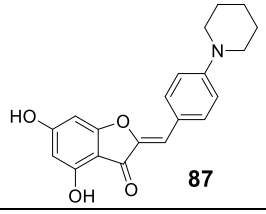 **87**	74 ± 5	≤ 20	≤ 20
5	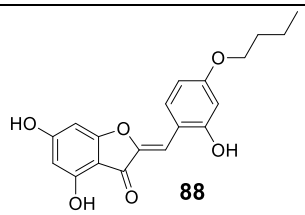 **88**	46 ± 6	-	-
6	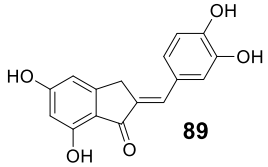 **89**	77 ± 1	≤ 20	23 ± 6
7	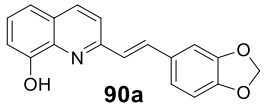 **90a**	93 ± 1	26 ± 8	79 ± 2

8	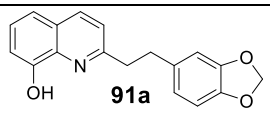 **91a**	90 ± 1	38 ± 1	71 ± 4
9	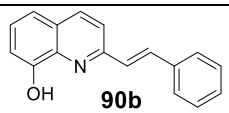 **90b**	95 ± 2	37 ± 12	84 ± 4
10	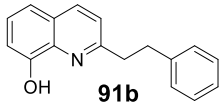 **91b**	85 ± 4	28 ± 7	76 ± 4

Inhibition constants were determined for selected active compounds, using a competitive model of inhibition. Interestingly, the K_i values measured for compounds **90b** and **91a** were found in the low micromolar range (2.2 ± 0.3 and 1.1 ± 0.2 µM, respectively), confirming the potent activity of such compounds. Remarkably, compounds **90b** also inhibited IMP-1 with a K_i value of 4.7 ± 0.5 µM, *i. e.* only roughly two-fold greater than that measured for NDM-1, and could thus represent an interesting scaffold for the optimization of broad-spectrum MBL inhibitors, by designing compounds whose activity on VIM-type enzymes would be improved.

These two compounds were also investigated for their ability to potentiate meropenem (a carbapenem antibiotic) in *in vitro* antimicrobial susceptibility assays on recent NDM-1-producing extensively-drug resistant *Klebsiella pneumoniae* clinical isolates, whose current global spread represents a worrisome issue. Interestingly, when tested at a fixed concentration of 32 µg/mL, compound **90b** was able to decrease the meropenem MIC 64- and 256-fold, depending on the strain tested (Table 2). Strikingly, the tested compounds also behaved very differently, as compound **91a** proved unable to even minimally affect the meropenem MIC, likely due to a much slower diffusion through the outer membrane, and thus a limited accumulation of the inhibitor in the bacterial periplasm.

Table 2. Evaluation of the *in vitro* antibacterial synergistic activity of compounds **90b** and **91a** (tested at a fixed concentration of 32 µg/mL) with meropenem on two epidemiologically unrelated NDM-1-producing *K. pneumoniae* and *E. coli* clinical isolates.

Compound	Meropenem MIC (µg/mL)	
	K. pneumonia SI-518	*E. coli* SI-004M
None	64	64
90b	0.25	1
91a	64	64

This underlines how relatively subtle chemical variations could lead to compounds potentially showing similar *in vitro* enzyme inhibition potencies, but remarkably different biological activities when tested in whole-cell assays. However, these data show that at least one of the compound described herein (**90b**) was able to inhibit two important subtypes of acquired MBLs (NDM-1 and IMP-1) but also to significantly potentiate the antibacterial activity of meropenem on contemporary ultra-resistant *Klebsiella pneumoniae* clinical isolates, with MICs in the presence of the inhibitor resulting below the

resistance breakpoint. Overall, these data provided valuable SAR information for further compound optimization, hopefully allowing the identification of additional potent NDM-1 inhibitors showing synergistic activity.

3. Conclusion

The FBDD methodology described in this article showed several advantages for the discovery and rational design of new NDM-1 inhibitors. Starting from high throughput virtual screening of large molecules on the zinc dinuclear enzyme, relevant fragments have been identified. They subsequently entered a broader in-house untargeted fragment library. This set of fragments (around 300) were screened by STD NMR and led to the identification of 37 fragments that could potentially be further developed by growing, linking or merging strategies to finally give fine-tuned NDM-1 inhibitors. Some of these fragments are known to interact with MBLs (even NDM-1 in some instances), proving the efficiency of our methodology to identify binders of NDM-1, but some of them possess original structure for further investigations. A pharmacophore study was led from these fragments and DFT calculation on 8-HQ allowed to propose 4 first analogues that were synthesized and showed *in vitro* inhibitory activity of NDM-1 in biochemical assays. Furthermore, with the same objective to validate our methodology, 2 aurones and 1 indenone, including 2-HAP, another fragment identified by the FBDD methodology, were obtained and evaluated. These compounds presented an *in vitro* inhibitory activity on NDM-1 and IMP-1, with inhibition constants in the low micromolar range for NDM-1. More strikingly, compound **90b** was able to potentiate the activity of meropenem up to 256-fold on NDM-1-producing *Klebsiella pneumoniae* contemporary clinical isolates, with meropenem MIC values (0.25-1 µg/mL) in the susceptibility range when combined with this compound. In conclusion, the different selectivity profile of aurone/indenone on the one hand and 8-HQ on the other hand are deemed interesting: our design methodology proved successful to find fragments potentially suitable to identify potent inhibitors on NDM-1, one of which showing significant synergistic antibacterial activity. Since it is now well recognized that the discovery and development of broad-spectrum MBL inhibitors would represent an urgent need to adequately address the global issue of antibiotic resistance, future work will now focus on the pharmacomodulation of these hits (especially the most promising **90b** to improve their activity on NDM-1, their inhibition profile on other relevant MBLs (*e. g.* IMP-, VIM-type enzymes) and physico-chemical properties adequate for rapid accumulation in the bacterial periplasm.

4. Experimental section

4.1. Virtual screening

Maestro was used to perform protein and ligand preparation, receptor grid generation, docking and pharmacophore analysis using Glide, LigPrep, Epik and Phase modules (Schrödinger, LLC, New York, NY, USA).

Molecules used for the virtual screening (770,000) were extracted from subset of ZINC15 [19], DrugBank [18] and French National library [17] in sdf format, shortlisted with reactive filter (708 404) and prepared with LigPrep. The ionization states of compounds were generated at pH 7 ± 1 with Epik. An OPLS3 force field [41] was used to minimize the energy of each compound with default parameters and finally obtain 857 701 structures.

The X-ray crystal structure of NDM-1 in complex with hydrolyzed ampicilin (PDB 5ZGE) [42] at a resolution of 1.00 Å was used. The protein was prepared using the protein preparation wizard of Glide. Crystallographic water molecules were removed while the catalytic hydroxide ion was kept intact. The grid box was generated by selecting the centre of the bound ligand as the centroid of the grid box of 30 Å side in the receptor-grid generation module of Maestro.

Glide was used for the two first steps of the docking. All the compounds were docked at the active site of NDM-1 using HTVS (High Throughput Virtual Screening) and compounds belonging to first 5 % of scores were kept. Extra precision (XP) docking was performed on compounds shortlisted after HTVS, the top 10 % of scores were kept. Post-docking analyses and visualization were performed on Maestro.

Docking with GOLD [22] was executed on Hermes interface and was used for the steps involved in the receptor grid generation and docking. Output NDM-1 structure from protein preparation wizard of Glide and output molecules from docking of Glide with XP precision were converted in mol2 format to fit with GOLD input. The grid was defined with wizard tool of Hermes as a sphere with a diameter of 30 Å centred on the hydroxide ion of the active site. For the docking, default parameters were used except for the Fitness option where ChemScore [43] was selected.

4.2. STD NMR Analyses

STD experiences have been performed at "Centre de RMN à Très Haut Champs" in Lyon (France). Samples were prepared with 8 µM of NDM-1 protein obtained from Sienna Lead Discovery in HEPES 10 mM at pH 7.5, NaCl 0.15 M and $ZnSO_4$ 50 µM. Fragment in DMSO-*d6* was added to the protein sample at a final concentration of 500 µM. Spectra were recorded at 20 °C with 16 scans for 1D spectra and 200 to 800 scans for STD spectra.

4.3. DFT calculations

All the DFT calculations were done using the Gaussian 16 program [44] with the MN15 global hybrid functional [45]. The latter was chosen for its ability to correctly describe weak interaction between the parts of the system without using an empirical dispersion correction term. The Def2-SVP [46,47] basis set was used for all atoms to optimize the geometries and calculate energies. Calculations (including geometry optimizations) were carried with an implicit model of solvent (PCM) [48], accounting for the polarization effects of the environment, considered as water. Binding energies were determined as the difference between the energy of the model protein/ligand complex and the sum of their internal energies when separate. All models are in their optimized geometries. The model of the active site was built using the PDB structure 5ZGE of NDM-1. The models include two zinc atoms and their coordinated amino acids (His_{120}, His_{122}, His_{189}, Asp_{124}, Cys_{208}, His_{250}), the HO^- cofactor and Lys_{211} which is involved in the substrate recognition. Only side chains of residues were kept, including α-carbons, replaced by methyl groups. In order to keep the local structure of the active site, α-carbons were kept fixed in their crystallographic positions, while the hydrogens bound to them (replacing the adjacent atoms) were free to move only along the Cα-N or Cα-C direction found in the crystallographic structure. By doing so, the Cα-Cβ bonds are allowed to move but are restrained to keep an orientation

similar to the original one. This approach has proven its efficiency in keeping the general shape of the active site [49]. Different kinds of system were studied: active site alone (Zn_2-OH^-), inhibitor alone or the complex of both. Calculation gave the following value where E stands for internal energy:
ΔE_1 = E(S1)–E(S0)–E(8HQ) = (–6325.0757)–(–5848.8272)–(–476.1937) = –0.0548 hartree = –34.4 kcal/mol
ΔE_2 = E(S2)–E(S1) = (–6325,0763)–(–6325.0757) = –0.0006 hartree = –0.4 kcal/mol
ΔE_3 = E(S3)–E(S2)+E(H_2O) = (–6248,7641)–(–6325.0757)+(–76,2795) = +0.0321 hartree = +20.1 kcal/mol

4.4. Chemistry

Unless specified, all reagents and solvents were used directly from commercial sources. Reaction progress was monitored by Thin Layer Chromatography (TLC) on aluminium backed silica gel MN 60 F254 plates from Macherey-Nagel. The synthesized products were mostly purified by column chromatography on silica gel (MN Kiesegel 60 silica gel mesh size 63-200 µm). Nuclear Magnetic Resonance (NMR) spectra were recorded at 25 °C on a Brucker UltraShield instrument (400 MHz for ^{1}H spectra, 101 MHz for ^{13}C spectra) in deuterated solvents. Chemical shifts (δ) are reported in parts per million (ppm) relative to the solvent [^{1}H: δ($CDCl_3$) = 7.26 ppm, δ(DMSO-d_6) = 2.50 ppm, δ(CD_3OD) = 3.31 ppm; ^{13}C: δ($CDCl_3$) = 77.2 ppm, δ(DMSO-d_6) = 39.5 ppm, δ(CD_3OD) = 49.0 ppm]. Multiplicity is reported as follows: bs, broad singlet; s, singlet; d, doublet; t, triplet and m, multiplet. Coupling constants *J* are given in Hertz. Electrospray Ionization (ESI) mass spectra and accurate mass measurements (HRMS) were acquired by NanoBio chemistry platform (ICMG FR2607). Specific optical rotation dispersion $[\alpha]_D$ were measured at 20 °C with a Perkin Elmer Polarimeter 341 apparatus. HPLC analyses were recorded on an Agilent 1100 series using a diode array detector and a C18 reversed-phase column (Nucleosil C18, Macherey-Nagel, 5 µm particle size, 125 mm × 3 mm) at 25 °C, with a mobile phase A composed of water and TFA 0.1 % and a phase mobile B composed of MeOH and TFA 0.1 % with a gradient 85:15 to 0:100 A:B over 10 min, 1 mL/min, 30 µL injection, detection at 254 nm. Purity of all the tested compounds was ≥ 95%.

*4.4.1. N-Benzyl-2-hydroxyacetamide (**13**)*. A suspension of glycolic acid **30** (100 mg, 1.32 mmol), benzylamine (0.17 mL, 1.58 mmol, 1.2 equiv), DCC (407 mg, 1.97 mmol, 1.5 equiv) and HOBt (355 mg, 2.63 mmol, 2.0 equiv) in CH_2Cl_2 (5 mL) was stirred at rt for 24 h. The reaction was quenched with saturated aqueous solution of $NaHCO_3$. The organic phase was washed with an aqueous solution of 1 M HCl, then with brine, dried over $MgSO_4$, filtered and concentrated *in vacuo*. The crude product was purified by silica gel column chromatography eluted with CH_2Cl_2/MeOH 995:5 to 985:15 to give the desired compound as a white solid (61 mg, 0.37 mmol, 28 %); Rf = 0.10 (cyclohexane/EtOAc 985:15); ^{1}H NMR (400 MHz, $CDCl_3$) δ ppm 7.39-7.23 (m, 5H), 6.96 (bs, 1H), 4.46 (s, 2H), 4.11 (s, 2H), 3.15 (bs, 1H). Analyses are in accordance with literature [50].

*4.4.2. L-Alanyl-L-phenylalanine TFA salt (**14a**)* – 2 steps
*4.4.2.1. Boc-L-alanyl-tBu-L-phenylalanine (**33**).* To a stirred suspension of L-phenylalanine *tert*-butyl ester chlorhydrate **31** (165 mg, 0.64 mmol, 1.2 equiv) in dry CH_2Cl_2 (6 mL) under N_2 atmosphere, were added EDC (152 mg, 0.79 mmol, 1.5 equiv), HOBt (71 mg, 0.53 mmol, 1.0 equiv), DMAP (6 mg, 0.05 mmol, 0.1 equiv) and *N*-Boc-L-Alanine (100 mg, 0.53 mmol, 1.0 equiv). At 0 °C, Et_3N (142 µL, 1.06 mmol, 2.0 equiv) was then added dropwise. The reaction was stirred at 0 °C for 30 min, then overnight at rt. The reaction was quenched with saturated aqueous solution of $NaHCO_3$. The organic phase was washed with a saturated aqueous solution of NH_4Cl, then with brine, dried over $MgSO_4$, filtered and

concentrated *in vacuo*. The crude product was purified by silica gel column chromatography eluted with cyclohexane/EtOAc 85:15 to 80:20 to give the desired compound as a white solid (135 mg, 0.34 mmol, 64 %); Rf = 0.50 (cyclohexane/EtOAc 6:4); ^{1}H NMR (400 MHz, $CDCl_3$) δ ppm 7.23-7.13 (m, 3H), 7.10-7.06 (m, 2H), 6.48 (d, *J* = 7.5 Hz, 1H), 5.04-4.86 (m, 1H), 4.64 (dt, *J* = 7.5, 6.0 Hz, 1H), 4.23-4.05 (m, 1H), 3.08-2.96 (m, 2H), 1.37 (s, 9H), 1.33 (s, 9H), 1.26 (d, *J* = 7.0 Hz, 3H); ^{13}C NMR (101 MHz, $CDCl_3$) δ ppm 172.2 (C), 170.4 (C), 155.4 (C), 136.2 (C), 129.7 (2xCH), 128.5 (2xCH), 127.1 (CH), 82.5 (C), 80.2 (C), 53.7 (CH), 50.2 (CH), 38.2 (CH_2), 28.4 (3xCH_3), 28.1 (3xCH_3), 18.6 (CH_3); LRMS (ESI+) *m/z* (%) 393 $[M+H]^+$ (100); HRMS (ESI+) *m/z* calc. for $C_{21}H_{32}N_2O_5Na$ 415.2203, found 415.2195 $[M+Na]^+$; $[\alpha]_D^{20}$ = + 13.9 ° (c = 1.00, CH_2Cl_2).

*4.4.2.2. L-Alanyl-L-phenylalanine TFA salt (**14a**)*. A solution of intermediate **33** (165 mg, 0.42 mmol, 1.0 equiv) in CH_2Cl_2/TFA 1:1 (4 mL) was stirred for 5 h at rt. The reaction mixture was concentrated *in vacuo*. The residue was dissolved in MeOH and concentrated again *in vacuo*, until precipitation. The precipitate was filtered to give the desired compound as a white solid (143 mg, 0.42 mmol, quantitative yield); ^{1}H NMR (400 MHz, CD_3OD) δ ppm 7.32-7.17 (m, 5H), 4.63 (dd, *J* = 9.1, 4.8 Hz, 1H), 3.85 (q, *J* = 7.0 Hz, 1H), 3.26 (dd, *J* = 14.0, 4.8 Hz, 1H), 3.00 (dd, *J* = 14.0, 9.1 Hz, 1H), 1.48 (d, *J* = 7.0 Hz, 3H); ^{13}C NMR (101 MHz, CD_3OD) δ ppm 175.1 (C), 170.8 (C), 138.8 (C), 130.3 (2xCH), 129.5 (2xCH), 127.8 (CH), 56.1 (CH), 50.2 (CH), 38.4 (CH_2), 17.6 (CH_3); LRMS (ESI+) *m/z* (%) 237 $[M+H]^+$ (100); HRMS (ESI+) *m/z* calc. for $C_{12}H_{17}N_2O_3$ 237.1233, found 237.1230 $[M+H]^+$; $[\alpha]_D^{20}$ = + 20.1 ° (c = 1.00, MeOH).

*4.4.3. 4-Acetyl-N-(piperidin-3-ylmethyl)benzamide TFA salt (**15a**)* – 2 steps

*4.4.3.1. tert-Butyl 3-((4-acetylbenzamido)methyl)piperidine-1-carboxylate (**36**).* To a stirred solution of 4-acetylbenzoic acid **34** (80 mg, 0.37 mmol, 1.0 equiv) in dry DMF (4 mL) under N_2 atmosphere, were added 3-(aminomethyl)-*N*-Boc-piperidine **35** (60 mg, 0.37 mmol, 1.0 equiv), TBTU (132 mg, 0.41 mmol, 1.1 equiv) and DIPEA (317 µL, 1.87 mmol, 5 equiv). After stirring at rt for 24 h, the reaction mixture was evaporated *in vacuo*. The residue was then dissolved in CH_2Cl_2 and washed with a saturated aqueous solution of $NaHCO_3$. The organic phase was washed with a saturated aqueous solution of NH_4Cl, dried over $MgSO_4$, filtered and concentrated *in vacuo*. The crude product was purified by silica gel column chromatography eluted with cyclohexane/EtOAc 6:4 to 4:6 to give the desired compound as a light yellow oil (130 mg, 0.36 mmol, 96 %); Rf = 0.21 (cyclohexane/EtOAc 1:1); ^{1}H NMR (400 MHz, $CDCl_3$) δ ppm 7.99 (d, *J* = 8.4 Hz, 2H), 7.89 (d, *J* = 8.4 Hz, 2H), 6.92 (s, 1H) 3.70-3.46 (m, 3H), 3.31-3.05 (m, 3H), 2.62 (s, 3H), 1.96-1.77 (m, 2H), 1.75-1.58 (m, 1H), 1.52-1.34 (m, 11H); ^{13}C NMR (101 MHz, $CDCl_3$) δ ppm 197.6 (C), 166.7 (C), 155.5 (C), 139.3 (C), 138.6 (C), 128.6 (2xCH), 127.4 (2xCH), 79.9 (C), 47.0 (CH_2), 45.2 (CH_2), 41.7 (CH_2), 35.4 (CH), 28.6 (CH_3), 28.2 (CH_2), 26.9 (CH_3), 23.4 (CH_2); LRMS (ESI+) *m/z* (%) 399 $[M+K]^+$ (100), 383 $[M+Na]^+$ (65), 361 $[M+H]^+$ (50); HRMS (ESI+) *m/z* calc. for $C_{20}H_{29}N_2O_4$ 361.2122, found 361.2117 $[M+H]^+$.

*4.4.3.2. 4-Acetyl-N-(piperidin-3-ylmethyl)benzamide TFA salt (**15a**).* Intermediate **36** (100 mg, 0.28 mmol, 1.0 equiv) was dissolved in a solution of CH_2Cl_2/TFA 1:1 (3 mL). The reaction was allowed to proceed for 5 h at rt. The reaction mixture was concentrated *in vacuo*. The product was dissolved in MeOH and concentrated again *in vacuo* until the residue turned to solid. The product was washed with cold CH_2Cl_2 to give the desired compound as a light yellow solid (93 mg, 0.21 mmol, 89 %); ^{1}H NMR (400 MHz, CD_3OD) δ ppm 8.07 (d, *J* = 8.5 Hz, 2H), 7.93 (d, *J* = 8.5 Hz, 2H), 3.44-3.26 (m, 4H), 2.93 (td, *J* = 12.7, 3.2 Hz, 1H), 2.76 (t, *J* = 12.1 Hz, 1H), 2.63 (s, 3H), 2.20-2.05 (m, 1H), 2.03-1.89 (m, 2H), 1.81-1.65 (m, 1H), 1.45-1.26 (m, 1H); ^{13}C NMR (101 MHz, CD_3OD) δ ppm 199.7 (C), 169.7 (C), 140.7 (C), 139.4 (C), 129.6 (2xCH), 128.7 (2xCH), 48.4 (CH_2), 45.4 (CH_2), 43.6 (CH_2), 36.0 (CH), 27.5 (CH_2), 26.9 (CH_3), 23.0 (CH_2); LRMS (ESI+) *m/z* (%) 261 $[M+H]^+$; HRMS (ESI+) *m/z* calc. for $C_{15}H_{21}N_2O_2$ 261.1597, found 261.1591 $[M+H]^+$.

*4.4.4. 2-((4-Hydroxyphenyl)carbamoyl)benzoic acid (**16**).* To a solution of 4-aminophenol (296 mg, 2.72 mmol, 1.0 equiv) in dry CH_2Cl_2 (3 mL), were added pyridine (0.56 mL, 6.76 mmol, 2.5 equiv) and a solution of anhydride phtalic **38** (400 mg, 2.72 mmol, 1.0 equiv) in 3 mL of dry CH_2Cl_2. The reaction mixture was stirred at rt for 15 h under N_2 atmosphere. The solid was filtered and dissolved in a saturated aqueous solution of $NaHCO_3$. The aqueous phase was washed with CH_2Cl_2 and acidified with HCl 1 M until pH = 1. Aqueous phase was extracted with EtOAc, organic phases were gathered, washed with brine, dried over $MgSO_4$, filtered and concentrated *in vacuo*. The product was washed with CH_2Cl_2 to give the desired compound as a light beige solid (187 mg, 0.73 mmol, 27 %); ^{1}H NMR (400 MHz, DMSO-d_6) δ ppm 12.87 (bs, 1H), 10.05 (s, 1H), 9.19 (s, 1H), 7.84 (d, *J* = 7.1 Hz, 1H), 7.63 (ddd, *J* = 7.4, 7.4, 0.9 Hz, 2H), 7.58-7.49 (m, 2H), 7.47 (d, *J* = 8.8 Hz, 2H), 6.72 (d, *J* = 8.8 Hz, 2H). Analyses are in accordance with literature [51].

*4.4.5. 3-((4-Methoxyphenyl)amino)-3-oxopropanoic acid (**17**).* Meldrum's acid **40** (200 mg, 1.39 mmol, 1.0 equiv) and 4-methoxyaniline **39** (170 mg, 1.39 mmol, 1.0 equiv) were refluxed in water (3 mL) for 2 h. The reaction mixture was cooled to rt and the precipitate was filtered. The product was dissolved in an aqueous 10 % KOH solution. The mixture was filtered again. The filtrate was cooled to 0 °C and a 1 M aqueous HCl solution was added. The precipitate was finally filtered to give the desired compound as a white solid (110 mg, 0.50 mmol, 38 %); ^{1}H NMR (400 MHz, DMSO-d_6) δ ppm 12.61 (bs, 1H), 9.99 (s, 1H), 7.48 (d, *J* = 8.9 Hz, 2H), 6.88 (d, *J* = 8.9 Hz, 2H), 3.71 (s, 3H), 3.30 (s, 2H, H2). Analyses are in accordance with literature [52].

*4.4.6. 2-(Hydroxy(phenylamino)methylene)-1H-indene-1,3(2H)-dione (**18**).* To a solution of indane-1,3-dione **41** (100 mg, 0.68 mmol, 1.0 equiv) and Et_3N (194 µL, 1.44 mmol, 2.1 equiv) in dry DMF, was added phenylisocyanate **42** (82 µL, 0.75 mmol, 1.1 equiv) at –35 °C. The reaction mixture was stirred at this temperature for 2 h under N_2 atmosphere. The mixture was diluted with water, an aqueous solution of HCl 1 M was added and the product was filtered and washed with MeOH to give the desired compound as a yellow solid (101 mg, 0.38 mmol, 56 %); Rf = 0.20 (CH_2Cl_2/MeOH 9:1); ^{1}H NMR (400 MHz, $CDCl_3$) δ ppm 9.54 (bs, 1H, NH), 7.97 (bs, 1H), 7.70-7.48 (m, 6H), 7.40 (t, *J* = 7.9 Hz, 2H), 7.22 (t, *J* = 7.4 Hz, 1H). Analyses are in accordance with literature [53].

*4.4.7. 1-(2-Aminoethyl)-3-phenylurea TFA salt (**19a**)* – 2 steps

*4.4.7.1. tert-Butyl (2-(3-phenylureido)ethyl)carbamate (**44**).* To a solution of Boc-ethylenediamine **43** (140 mg, 0.88 mmol, 1.0 equiv) in CH_2Cl_2 (5 mL), was added phenylisocyanate **42** (96 µL, 0.88 mmol, 1.0 equiv). The reaction mixture was stirred at rt for 2 h. The precipitate was filtered and washed with cold CH_2Cl_2 to give the desired compound as a white solid (179 mg, 0.64 mmol, 73 %); ^{1}H NMR (400 MHz, DMSO-d_6) δ ppm 8.50 (bs, 1H), 7.37 (d, *J* = 7.8 Hz, 2H), 7.20 (dd, *J* = 7.8, 7.8 Hz, 2H), 6.94-6.80 (m, 2H), 6.14 (t, *J* = 4.9 Hz 1H), 3.17-3.07 (m, 2H), 3.05-2.95 (m, 2H), 1.38 (s, 9H). Analyses are in accordance with literature [54].

*4.4.7.2. 1-(2-Aminoethyl)-3-phenylurea TFA salt (**19a**).* Intermediate **44** (80 mg, 0.29 mmol, 1.0 equiv) was dissolved in a solution of CH_2Cl_2/TFA 1:1 (3 mL). The reaction was allowed to proceed for 5 h at rt. The reaction mixture was concentrated *in vacuo*. The product was dissolved in MeOH and concentrated again *in vacuo* until the residue turned to solid to give the desired compound as a white solid (84 mg, 0.29 mmol, quantitative yield); ^{1}H NMR (400 MHz, CD_3OD) δ ppm 7.41-7.35 (m, 2H), 7.28-7.22 (m, 2H), 7.02-6.96 (m, 1H), 3.47 (t, *J* = 5.8 Hz, 2H), 3.07 (t, *J* = 5.8 Hz, 2H); ^{13}C NMR (101 MHz, CD_3OD) δ ppm 158.9 (C), 140.6 (C), 129.8 (2xCH), 123.8 (CH), 120.5 (2xCH), 41.7 (CH_2), 38.8 (CH_2); LRMS (ESI+) *m/z* (%) 180 $[M+H]^+$ (100); HRMS (ESI+) *m/z* calc. for $C_9H_{14}N_3O$ 180.1132, found 180.1132 $[M+H]^+$.

*4.4.8. trans-2-Phenoxycyclohexanol (**20**).* To a solution of *t*BuOK (137 mg, 1.22 mmol, 1.2 equiv) in THF/*t*BuOH 1:1 (4 mL), was added phenol (106 mg, 1.12 mmol, 1.1 equiv). The reaction mixture was stirred for 10 min under N_2 atmosphere then cyclohexene oxide **45** (103 µL, 1.02 mmol, 1.0 equiv) was added dropwise and the reaction was refluxed for 3 days. The solution was cooled to rt, the precipitate was filtered off and the filtrate was concentrated *in vacuo*. The crude product was dissolved in ether, washed with a 20 % aqueous solution of NaOH then with brine. The organic phase was dried over $MgSO_4$, filtered and concentrated *in vacuo* to give the desired compound as a white solid (87 mg, 0.45 mmol, 44 %); Rf = 0.30 (cyclohexane/EtOAc 8:2); ^{1}H NMR (400 MHz, $CDCl_3$) δ ppm 7.24-7.16 (m, 2H), 6.92-6.84 (m, 3H), 3.92 (ddd, *J* = 10.2, 8.5, 4.6 Hz, 1H), 3.65 (ddd, *J* = 10.6, 8.5, 4.6 Hz, 1H), 2.41 (bs, 1H), 2.12-1.99 (m, 2H), 1.74-1.59 (m, 2H), 1.40-1.13 (m, 4H). Analyses are in accordance with literature [55].

*4.4.9. 4-(2-(Pyrrolidin-1-yl)ethoxy)phenol (**21**)* – 2 steps

*4.4.9.1. 1-(2-(4-(Benzyloxy)phenoxy)ethyl)pyrrolidine (**49**).* To a solution of 4-benzyloxyphenol **47** (518 mg, 1.59 mmol, 1.1 equiv) and 1-(2-chloroethyl)pyrrolidine hydrochloride **48** (400 mg, 2.35 mmol, 1.0 equiv) in DMF (15 mL), were added K_2CO_3 (130 mg, 0.94 mmol, 1.6 equiv) and Cs_2CO_3 (210 mg, 0.65 mmol, 1.1 equiv). The reaction mixture was stirred at rt for 3 days, then water was added and the aqueous phase was extracted with CH_2Cl_2. Organic phases were gathered, washed with a saturated aqueous solution of $NaHCO_3$ then with brine, dried over $MgSO_4$, filtered and concentrated *in vacuo*. The crude product was purified by silica gel column chromatography eluted with CH_2Cl_2/MeOH 95:5 to 90:10 to give the desired compound as a light yellow solid (62 mg, 0.21 mmol, 35 %); Rf = 0.22 (CH_2Cl_2/MeOH 9:1); ^{1}H NMR (400 MHz, $CDCl_3$) δ ppm 7.46-7.28 (m, 5H), 6.94-6.83 (m, 4H), 5.01 (s, 2H), 4.08 (t, *J* = 5.8 Hz, 2H), 2.91 (t, *J* = 5.8 Hz, 2H), 2.72-2.64 (m, 4H), 1.90-1.82 (m, 4H); ^{13}C NMR (101 MHz, $CDCl_3$) δ ppm 153.3 (C), 153.1 (C), 137.4 (2xCH), 128.6 (C), 127.9 (CH), 127.5 (2xCH), 115.9 (2xCH), 115.6 (2xCH), 70.7 (CH_2), 67.6 (CH_2), 55.2 (CH_2), 54.8 (2xCH_2), 23.6 (2xCH_2); LRMS (ESI+) *m/z* (%) 298 $[M+H]^+$ (100); HRMS (ESI+) *m/z* calc. for $C_{19}H_{24}NO_2$ 298.1802, found 298.1947 $[M+H]^+$.

*4.4.9.2. 4-(2-(Pyrrolidin-1-yl)ethoxy)phenol (**21**).* To a suspension of activated Pd/C 10 % (23 mg, 0.02 mmol, 0.1 equiv) in absolute EtOH (3 mL) was added compound **49** (65 mg, 0.22, mmol, 1.0 equiv). The reaction mixture was stirred at rt for 24 h under H_2 atmosphere, then filtered on a pad of Celite®. The filtrate was evaporated and the crude product was purified by silica gel column chromatography (CH_2Cl_2/MeOH 97:3 to 90:10) to give the desired compound as an orange solid (28 mg, 0.14 mmol, 61 %); Rf = 0.20 (CH_2Cl_2/MeOH 9:1); ^{1}H NMR (400 MHz, CD_3OD) δ ppm 6.85-6.79 (m, 2H), 6.74-6.69 (m, 2H), 4.13 (t, *J* = 5.2 Hz, 2H), 3.24 (t, *J* = 5.2 Hz, 2H), 3.06 (t, *J* = 6.0 Hz, 4H), 2.04-1.93 (m, 4H); ^{13}C NMR (101 MHz, CD_3OD) δ ppm 153.0 (C), 152.9 (C), 116.9 (2xCH), 116.8 (2xCH), 66.7 (CH_2), 55.8 (CH_2), 55.6 (2xCH_2), 24.1 (2xCH_2); LRMS (ESI+) *m/z* (%) 208 $[M+H]^+$ (100); HRMS (ESI+) *m/z* calc. for $C_{12}H_{18}NO_2$ 208.1323, found 208.1333 $[M+H]^+$.

*4.4.10. N-(2-(Dimethylamino)ethyl)thiophene-2-sulfonamide (**24**).* To a solution of *N*,*N*-dimethylethylenediamine **51** (103 µL, 0.99 mmol, 1.2 equiv) in dry CH_2Cl_2 (8 mL), were added Et_3N (332 µL, 2.47 mmol, 3 equiv) and 2-thiophenesulfonyl chloride **50** (150 mg, 0.82 mmol, 1.0 equiv) . The reaction mixture was stirred at rt for 48 h then quenched with a saturated aqueous solution of $NaHCO_3$. The organic phase was washed with an aqueous solution of 1 M HCl, then with brine, dried over $MgSO_4$, filtered and concentrated *in vacuo*. The crude product was purified by silica gel column chromatography eluted with CH_2Cl_2/MeOH 95:5 to give the desired compound as a colourless oil (137 mg, 0.59 mmol, 71 %); Rf = 0.29 (CH_2Cl_2/MeOH 8:2); ^{1}H NMR (400 MHz, $CDCl_3$) δ ppm 7.63 (dd, *J* = 3.7, 1.3 Hz, 1H), 7.58 (dd, *J* = 5.0, 1.3 Hz, 1H), 7.09 (dd, *J* = 5.0, 3.7 Hz, 1H), 3.10 (t, *J* = 5.5 Hz, 2H), 2.46 (t, *J* = 5.5 Hz, 2H), 2.19-2.15 (m, 6H); ^{13}C NMR (101 MHz, $CDCl_3$) δ ppm 140.8 (C), 132.3 (CH), 131.9 (CH),

127.5 (CH), 57.0 (CH_2), 44.7 (2xCH_3), 40.3 (CH_2); LRMS (ESI+) *m/z* (%) 235 $[M+H]^+$ (100); HRMS (ESI+) *m/z* calc. for $C_8H_{15}N_2O_2S_2$ 235.0570, found 235.0572 $[M+H]^+$.

*4.4.11. N,N-Dimethyl-1-phenyl-1-(2H-tetrazol-5-yl)methanamine (**25**)* – 2 steps

*4.4.11.1. 2-(Dimethylamino)-2-phenylacetonitrile (**53**).* To a solution of *N*,*N*-dimethylbenzamide **52** (250 mg, 1.68 mmol, 1.0 equiv) in dry toluene, was added (17 mL) Vaska's complex $[IrCl(CO)(Ph_3P)_2]$ (13 mg, 0.02 mmol, 0.01 equiv). The solution was stirred at rt under N_2 atmosphere during 5 min then 1,1,3,3-tetramethyldisiloxane (TMDS, 592 µL, 3.36 mmol, 2.0 equiv) was added. The reaction mixture was stirred until the solution turned colourless. TMSCN (421 µL, 3.36 mmol, 2.0 equiv) was then added and the reaction was stirred at rt for 15 h. The reaction mixture was treated with an aqueous solution of 1 M NaOH and the aqueous phase was extracted with EtOAc. Organic phases were gathered, dried over $MgSO_4$, filtered and concentrated *in vacuo*. The crude product was purified by silica gel column chromatography eluted with cyclohexane/EtOAc 1:9 to give the desired compound as a light-yellow oil (227 mg, 1.42 mmol, 85 %); Rf = 0.40 (cyclohexane/EtOAc 8:2); ^{1}H NMR (400 MHz, $CDCl_3$) δ ppm 7.56-7.50 (m, 2H), 7.44-7.35 (m, 3H), 4.87 (s, 1H), 2.34 (s, 6H). Analyses are in accordance with literature [26].

*4.4.11.2. N,N-Dimethyl-1-phenyl-1-(2H-tetrazol-5-yl)methanamine (**25**).* To a solution of compound **53** (70 mg, 0.44 mmol, 1.0 equiv) in toluene (4 mL), were added trimethylsilylazide ($TMSN_3$, 572 µL, 4.38 mmol, 10 equiv) and dibutyltin oxide (65 mg, 0.26 mmol, 0.6 equiv). The reaction mixture was stirred at 70 °C for 3 days, EtOAc was added and the resulting precipitate was filtered off and washed with cold CH_2Cl_2 to give the desired compound as a white solid (36 mg, 0.18 mmol, 41 %); ^{1}H NMR (400 MHz, CD_3OD) δ ppm 7.70-7.64 (m, 2H), 7.51-7.42 (m, 3H), 5.76 (s, 1H), 2.78 (s, 6H). Analyses are in accordance with literature [26].

*4.4.12. Benzo[b]thiophene-2-carboximidamide hydrochloride (**26a**) – 2 steps*

*4.4.12.1. Methyl benzo[b]thiophene-2-carboxylate (**56**).* To a suspension of K_2CO_3 (668 mg, 4.84 mmol, 1.0 equiv) in DMF (10 mL), was added 2-fluorobenzaldehyde **54** (509 µL, 4.84 mmol, 1.0 equiv). After stirring at rt for 30 min under N_2 atmosphere, methyl thioglycolate **55** (441 µL, 4.84 mmol, 1.0 equiv) was added dropwise. The solution was then stirred at 90 °C for 2 h. The reaction mixture was cooled to rt then ice was added and the resulting precipitate was filtered off and purified by silica gel column chromatography eluted with cyclohexane/EtOAc 9:1 to give the desired compound as a light yellow solid (90 mg, 0.47 mmol, 39 %); Rf = 0.63 (cyclohexane/EtOAc 8:2); ^{1}H NMR (400 MHz, $CDCl_3$) δ ppm 8.07 (s, 1H), 7.89-7.84 (m, 2H), 7.48-7.37 (m, 2H), 3.95 (s, 3H). Analyses are in accordance with literature [56].

*4.4.12.2. Benzo[b]thiophene-2-carboximidamide hydrochloride (**26a**)*. To a suspension of ammonium chloride (123 mg, 2.29 mmol, 4 equiv) in toluene (3 mL) was added dropwise a solution of trimethylaluminum 2 M in hexane (0.58 mL, 2.29 mmol, 4 equiv). After stirring under N_2 at 0 °C for 30 min and at rt for another 30 min, compound **56** (110 mg, 0.57 mmol, 1.0 equiv) was added. The reaction mixture was refluxed for 4 h, then cooled to rt and filtered on a pad of silica eluted with CH_2Cl_2/MeOH 1:1. The filtrate was concentrated *in vacuo* and the crude product was purified by silica gel column chromatography eluted with CH_2Cl_2/MeOH 9:1 to give the desired compound as a light yellow solid (103 mg, 0.48 mmol, 85 %); Rf = 0.55 (CH_2Cl_2/MeOH 8:2); ^{1}H NMR (400 MHz, DMSO-d_6) δ ppm 9.54 (bs, 4H), 8.45 (d, *J* = 0.4 Hz, 1H), 8.23-8.16 (m, 1H), 8.10-8.03 (m, 1H), 7.63-7.57 (m, 1H), 7.57-7.51 (m, 1H); ^{13}C NMR (100MHz, DMSO-d_6) δ ppm 159.7 (C), 140.6 (C), 137.9 (C), 131.2 (CH), 129.0 (C), 127.9 (CH), 125.8 (CH), 123.1 (CH); LRMS (ESI+) *m/z* (%) 177 $[M+H]^+$ (100); HRMS (ESI+) m/z calc. for $C_9H_9N_2S$ 177.0481, found 177.0480 $[M+H]^+$.

*4.4.13. 2-Cyano-1-propyl-3-(pyridin-3-yl)guanidine (**27**)* – 2 steps

*4.4.13.1. Methyl pyridin-3-yl cyanocarbonimidodithioate (**59**).* To a solution of 3-aminopyridine **57** (500 mg, 5.32 mmol, 1.0 equiv) and dimethyl *N*-cyanodithioiminocarbonate **58** (932 mg, 6.38 mmol, 1.2 equiv) in DMF (4 mL), was added at 0 °C a suspension of NaH 60 % in oil (319 mg, 7.98 mmol, 7.98 equiv). The reaction mixture was stirred at 50 °C for 6 h, then water (20 mL) and AcOH (0.7 mL) were added at 0 °C. The precipitate was filtered off, washed with water and cold CH_2Cl_2 to give the desired compound as a white solid (376 mg, 1.96 mmol, 37 %); Rf = 0.45 (CH_2Cl_2/MeOH 9:1); ^{1}H NMR (400 MHz, DMSO-d_6) δ ppm 10.26 (bs, 1H), 8.62 (s, 1H), 8.43 (d, *J* = 4.2 Hz, 1H), 7.89 (d, *J* = 8.0 Hz, 1H), 7.44 (dd, *J* = 8.0, 4.2 Hz, 1H), 2.73 (s, 3H). Analyses are in accordance with literature [57].

*4.4.13.2. 2-Cyano-1-propyl-3-(pyridin-3-yl)guanidine (**27**).* To a solution of propylamine (516 µL, 6.30 mmol, 10 equiv) in dry pyridine (1.5 mL), was added methyl compound **59** (120 mg, 0.63 mmol, 1.0 equiv). The reaction mixture was stirred at rt for 4 days under N_2 atmosphere. After concentration *in vacuo*, the residue was suspended in water. The precipitate was filtered off and washed with water to give the desired compound as a white solid (56 mg, 0.28 mmol, 44 %); ^{1}H NMR (400 MHz, DMSO-d_6) δ ppm 9.05 (bs, 1H), 8.46 (s, 1H), 8.33 (d, *J* = 4.2 Hz, 1H), 7.67 (d, *J* = 8.0 Hz, 1H), 7.44 (t, *J* = 5.6 Hz, 1H), 7.37 (dd, *J* = 8.0, 4.2 Hz, 1H), 3.23-3.14 (m, 2H), 1.58-1.47 (m, 2H), 0.87 (t, *J* = 7.4 Hz, 3H); ^{13}C NMR (101 MHz, DMSO-d_6) δ ppm 158.0 (C), 145.4 (CH), 144.4 (CH), 134.6 (C), 130.9 (CH), 123.6 (CH), 117.0 (C), 43.2 (CH_2), 22.1 (CH_2), 11.1 (CH_3); LRMS (ESI+) *m/z* (%) 204 $[M+H]^+$ (100); HRMS (ESI+) *m/z* calc. for $C_{10}H_{14}N_5$ 204.1244, found 204.1244 $[M+H]^+$.

*4.4.14. General procedure A for the synthesis of compounds **94a-b***

To a solution of 2-methyl-8-hydroxyquinoline **92** (1.0 equiv) in Ac_2O (2 mL/mmol), was added the benzaldehyde derivative (1.0 to 2.0 equiv). The reaction mixture was stirred at 130 °C for 24 h under N_2 atmosphere, then cooled to rt and diluted with water. The aqueous phase was extracted with EtOAc, organic phases were gathered, washed with brine, dried over $MgSO_4$, filtered and concentrated *in vacuo*. The crude product was purified by silica gel column chromatography. If necessary, the product was washed with cold MeOH.

*4.4.14.1. (E)-2-(2-(Benzo[d][1,3]dioxol-5-yl)vinyl)quinolin-8-yl acetate (**94a**).* The product was prepared following the general procedure A, starting from piperonal **93a** (377 mg, 2.52 mmol, 2 equiv) to give after column chromatography (cyclohexane/EtOAc 9:1) the desired compound as a yellow solid (120 mg, 0.36 mmol, 14 %); Rf = 0.29 (cyclohexane/EtOAc 7:3); ^{1}H NMR (400 MHz, DMSO-d_6) δ ppm 8.39 (d, *J* = 8.6 Hz, 1H), 7.87-7.81 (m, 2H), 7.75 (d, *J* = 16.2 Hz, 1H), 7.60-7.47 (m, 2H), 7.44 (d, *J* = 1.1 Hz, 1H), 7.33 (d, *J* = 16.2 Hz, 1H), 7.19 (dd, *J* = 8.0, 1.1 Hz, 1H), 6.98 (d, *J* = 8.0 Hz, 1H), 6.09 (s, 2H), 2.50 (s, 3H); ^{13}C NMR (101 MHz, DMSO-d_6) δ ppm 169.4 (C), 155.5 (C), 148.1 (C), 148.1 (C), 146.9 (C), 140.1 (C), 136.7 (CH), 134.7 (CH), 130.5 (C), 128.1 (C), 126.5 (CH), 125.7 (CH), 125.6 (CH), 123.3 (CH), 121.7 (CH), 120.6 (CH), 108.5 (CH), 106.0 (CH), 101.4 (CH_2), 20.7 (CH_3); LRMS (ESI+) *m/z* (%) 334 $[M+H]^+$ (100); HRMS (ESI+) *m/z* calc. for $C_{20}H_{16}NO_4$ 334.1074, found 334.1082 $[M+H]^+$.

*4.4.14.2. (E)-2-Styrylquinolin-8-yl acetate (**94b**).* The product was prepared following the general procedure A, starting from benzaldehyde (133 mg, 1.26 mmol, 1.0 equiv) to give after column chromatography (cyclohexane/EtOAc 9:1) the desired compound as a yellow solid (141 mg, 0.49 mmol, 78 %); Rf = 0.52 (cyclohexane/EtOAc 7:3); ^{1}H NMR (400 MHz, $CDCl_3$) δ ppm 8.15 (d, *J* = 8.6 Hz, 1H), 7.73-7.59 (m, 5H), 7.54-7.31 (m, 6H), 2.59 (s, 3H). Analyses are in accordance with literature [58].

*4.4.15. General procedure B for the synthesis of compounds **90a-b***

To a solution of EtOH/HCl 37 %: 85/15 (10 mL/mmol), was added quinolin-8-yl acetate derivative **94a-b**. The reaction mixture was refluxed for 2 h, then cooled to rt, diluted with water and neutralized with a saturated aqueous solution of $NaHCO_3$ until pH = 7. The aqueous phase was extracted with CH_2Cl_2,

organic phases were gathered, washed with brine, dried over $MgSO_4$, filtered and concentrated *in vacuo*. The crude product was purified by silica gel column chromatography.

*4.4.15.1. (E)-2-(2-(benzo[d][1,3]dioxol-5-yl)vinyl)-8-hydroxyquinoline (**90a**).* The product was prepared following the general procedure B, starting from **94a** (110 mg, 0.33 mmol) to give after column chromatography (cyclohexane/EtOAc 94:6) the desired compound as a yellow solid (84 mg, 0.29 mmol, 87 %); Rf = 0.47 (cyclohexane/EtOAc 7:3); ^{1}H NMR (400 MHz, DMSO-d_6) δ ppm 9.49 (s, 1H), 8.26 (d, *J* = 8.6 Hz, 1H), 8.05 (d, *J* = 16.1 Hz, 1H), 7.70 (d, *J* = 8.6 Hz, 1H), 7.40-7.30 (m, 4H), 7.17 (dd, *J* = 8.0, 1.5 Hz, 1H), 7.08 (dd, *J* = 6.9, 1.9 Hz, 1H), 6.99 (d, *J* = 8.0 Hz, 1H), 6.08 (s, 2H); ^{13}C NMR (101 MHz, DMSO-d_6) δ ppm 153.6 (C), 152.8 (C), 148.0 (C), 147.8 (C), 138.1 (C), 136.4 (CH), 134.2 (CH), 131.0 (C), 127.5 (C), 126.8 (CH), 126.1 (CH), 122.9 (CH), 120.9 (CH), 117.5 (CH), 111.1 (CH), 108.6 (CH), 105.7 (CH), 101.3 (CH_2); LRMS (ESI+) m/z (%) 292 $[M+H]^+$ (100); HRMS (ESI+) m/z calc. for $C_{18}H_{14}NO_3$ 292.0968, found 292.0972 $[M+H]^+$.

*4.4.15.2. (E)-2-Styryl-8-hydroxyquinoline (**90b**).* The product was prepared following the general procedure B, starting from **94b** (70 mg, 0.24 mmol) to give after column chromatography (cyclohexane/EtOAc 94:6) the desired compound as a yellow solid (48 mg, 0.19 mmol, 81 %); Rf = 0.67 (cyclohexane/EtOAc 7:3); ^{1}H NMR (400 MHz, $CDCl_3$) δ ppm 8.10 (d, *J* = 8.6 Hz, 1H), 7.71 (d, *J* = 16.3 Hz, 1H), 7.65-7.60 (m, 3H), 7.45-7.33 (m, 5H), 7.29 (dd, *J* = 8.2, 1.2 Hz, 1H), 7.19 (dd, *J* = 7.6, 1.2 Hz, 1H). Analyses are in accordance with literature [58].

*4.4.16. General procedure C for the synthesis of compounds **91a-b***

To a suspension of activated Pd/C 10 (0.1 equiv) in EtOAc (10 mL/mmol) was added compound **90a-b** (1.0 equiv). The reaction mixture was stirred at rt for 24 h under H_2 atmosphere, then filtered on a pad of diatomaceous earth. The filtrate was evaporated and the crude product was purified by silica gel column chromatography.

*4.4.16.1. 2-(2-(Benzo[d][1,3]dioxol-5-yl)ethyl)-8-hydroxyquinoline (**91a**).* The product was prepared following the general procedure C, starting from compound **90a** (50 mg, 0.17 mmol) to give after column chromatography (cyclohexane/EtOAc 9:1) the desired compound as a light yellow oil (27 mg, 0.09 mmol, 54 %); Rf = 0.47 (cyclohexane/EtOAc 8:2); ^{1}H NMR (400 MHz, $CDCl_3$) δ ppm 8.05 (d, *J* = 8.4 Hz, 1H), 7.41 (dd, *J* = 8.2, 7.6 Hz, 1H), 7.29 (dd, *J* = 8.2, 1.2 Hz, 1H), 7.25 (d, *J* = 8.4 Hz, 1H), 7.18 (dd, *J* = 7.6, 1.2 Hz, 1H), 6.75-6.70 (m, 2H), 6.66 (dd, *J* = 7.9, 1.7 Hz, 1H), 5.92 (s, 2H), 3.26 (dd, *J* = 9.0, 6.4 Hz, 2H), 3.10 (dd, *J* = 9.2, 6.4 Hz, 2H); ^{13}C NMR (101 MHz, $CDCl_3$) δ ppm 159.5 (C), 151.8 (C), 147.8 (CH), 145.9 (C), 137.5 (C), 136.7 (CH), 135.3 (C), 127.1, 127.1 (CH, C), 122.5 (CH), 121.4 (CH), 117.8 (CH), 110.4 (CH), 109.0 (CH), 108.3 (CH), 100.9 (CH_2), 40.3 (CH_2), 35.2 (CH_2); LRMS (ESI+) m/z (%) 294 $[M+H]^+$ (100); HRMS (ESI+) m/z calc. for $C_{18}H_{16}NO_3$ 294.1125, found 294.1123 $[M+H]^+$.

*4.4.16.2. 2-Phenethyl-8-hydroxyquinoline (**91b**).* The product was prepared following the general procedure C, starting from compound **90b** (50 mg, 0.20 mmol) to give after column chromatography (cyclohexane/EtOAc 94:6) the desired compound as a light yellow oil (32 mg, 0.19 mmol, 64 %); Rf = 0.67 (cyclohexane/EtOAc 7:3); ^{1}H NMR (400 MHz, $CDCl_3$) δ ppm 7.93 (d, *J* = 8.4 Hz, 1H), 7.33-7.27 (m, 1H), 7.22-7.06 (m, 8H), 3.24-3.17 (m, 2H), 3.11-3.05 (m, 2H). Analyses are in accordance with literature [59].

4.5. Enzyme inhibition assays

The NDM-1 and IMP-1 metallo-β-lactamases were produced and purified as previously described [60]. The inhibitory activity of synthesized compounds was evaluated using spectrophotometric assays and

the reporter substrate method, as previously described [59]. The hydrolysis rate of imipenem (used as the reporter substrate, final concentration 150 µM) was monitored by following the time-dependence variation of absorbance (300 nm) in both the absence and presence of compounds, in 50 mM HEPES buffer (pH 7.5). Compounds were initially resuspended in DMSO (100 mM) and subsequently diluted in the reaction buffer. The percentage of inhibition on NDM-1 was computed using the following formula: 100 - [100 × (v_i / v_0)], where v_0 and v_i are the hydrolysis rates of the reporter substrate in the absence and presence of 50 µM compound, respectively. 5 mM EDTA was used as an inhibition control in these experiments.
Similarly, inhibition constants (K_i values) were determined using a competitive inhibition model by measuring the initial reaction rate of hydrolysis of the reporter substrate (150 µM imipenem) in 50 mM HEPES buffer (pH, 7.5) by means of spectrophotometric assays, in the absence and presence of a variable concentration of inhibitor and by plotting the v_0 / v_i ratio *vs* compound concentration:

$$\frac{v_0}{v_i} = \frac{K_M}{(K_M + [S])\, K_i} \cdot [I]$$

where [S] is the concentration of reporter substrate, [I] the concentration of the tested compound and K_M the Michaelis constant of the enzyme for the reporter substrate. K_i values computed as K_M / [(K_M + [S]) slope]. All assays were performed in triplicate.

4.5. In vitro *antimicrobial susceptibility testing*

The potential synergistic activity of selected compounds was evaluated on *K. pneumoniae* and *E. coli* NDM-1-producing clinical isolates (strains SI-518 and SI-004M) [61] by measuring the minimum inhibitory concentrations (MICs) of meropenem in both the absence and presence of a fixed concentration (32 µg/mL) of an inhibitor. MICs were determined in triplicate using Mueller-Hinton broth and a bacterial inoculum of 5 × 10^4 CFU/well, as recommended by the CLSI [62]. The stock solutions of the antibiotic (1.2 mg/mL in sterile milliQ water) and compounds (3.2 mg/mL in DMSO) were diluted in the growth medium. For assessing the activity of the combination, the inhibitor was added at 32 µg/mL to the wells immediately prior to the addition of the antibiotic diluted in growth medium containing 32 µg/mL inhibitor and the two-fold serial dilutions. Bacterial suspensions were added extemporaneously to each well, prior to incubation of the plates at 35 °C for 24 h. Results were read following visual inspection of the plates.

Declaration of Competing Interest

The authors declare no known competing interests that could have influence the work reported here.

Acknowledgments

The work presented here is dedicated to the memory of our colleague and friend Serge Crouzy who took a large and active part in this project, especially for the virtual screening work.

This work has been partially supported by Labex Arcane and CBH-EUR-GS (ANR-17-EURE-0003). The authors wish to acknowledge the ICMG Nanobio Platform (FR 2607), on which the NMR and MS experiment were performed.

Appendix A. Supplementary data

Supplementary data related to this article can be found at doi

References

[1] D.A. Erlanson, Introduction to Fragment-Based Drug Discovery, in: T.G. Davies, M. Hyvönen (Eds.), Fragm.-Based Drug Discov. X-Ray Crystallogr., Springer Berlin Heidelberg, Berlin, Heidelberg, 2012: pp. 1–32. https://doi.org/10.1007/128_2011_180.

[2] G.S. Basarab, J.I. Manchester, S. Bist, P.A. Boriack-Sjodin, B. Dangel, R. Illingworth, B.A. Sherer, S. Sriram, M. Uria-Nickelsen, A.E. Eakin, Fragment-to-Hit-to-Lead Discovery of a Novel Pyridylurea Scaffold of ATP Competitive Dual Targeting Type II Topoisomerase Inhibiting Antibacterial Agents, J. Med. Chem. 56 (2013) 8712–8735. https://doi.org/10.1021/jm401208b.

[3] D. Rognan, Fragment-Based Approaches and Computer-Aided Drug Discovery, in: T.G. Davies, M. Hyvönen (Eds.), Fragm.-Based Drug Discov. X-Ray Crystallogr., Springer Berlin Heidelberg, Berlin, Heidelberg, 2011: pp. 201–222. https://doi.org/10.1007/128_2011_182.

[4] I.J.P. de Esch, D.A. Erlanson, W. Jahnke, C.N. Johnson, L. Walsh, Fragment-to-Lead Medicinal Chemistry Publications in 2020, J. Med. Chem. 65 (2022) 84–99. https://doi.org/10.1021/acs.jmedchem.1c01803.

[5] C.L. Ventola, The Antibiotic Resistance Crisis, Pharm. Ther. 40 (2015) 277–283.

[6] M.-R. Meini, L.I. Llarrull, A.J. Vila, Overcoming differences: The catalytic mechanism of metallo-β-lactamases, FEBS Lett. 589 (2015) 3419–3432. https://doi.org/10.1016/j.febslet.2015.08.015.

[7] WHO publishes list of bacteria for which new antibiotics are urgently needed, (n.d.). https://www.who.int/news/item/27-02-2017-who-publishes-list-of-bacteria-for-which-new-antibiotics-are-urgently-needed (accessed September 1, 2021).

[8] R.P. Ambler, J. Baddiley, E.P. Abraham, The structure of β-lactamases, Philos. Trans. R. Soc. Lond. B Biol. Sci. 289 (1980) 321–331. https://doi.org/10.1098/rstb.1980.0049.

[9] D. Yong, M.A. Toleman, C.G. Giske, H.S. Cho, K. Sundman, K. Lee, T.R. Walsh, Characterization of a new metallo-beta-lactamase gene, bla(NDM-1), and a novel erythromycin esterase gene carried on a unique genetic structure in Klebsiella pneumoniae sequence type 14 from India, Antimicrob. Agents Chemother. 53 (2009) 5046–5054. https://doi.org/10.1128/AAC.00774-09.

[10] K.K. Kumarasamy, M.A. Toleman, T.R. Walsh, J. Bagaria, F. Butt, R. Balakrishnan, U. Chaudhary, M. Doumith, C.G. Giske, S. Irfan, P. Krishnan, A.V. Kumar, S. Maharjan, S. Mushtaq, T. Noorie, D.L. Paterson, A. Pearson, C. Perry, R. Pike, B. Rao, U. Ray, J.B. Sarma, M. Sharma, E. Sheridan, M.A. Thirunarayan, J. Turton, S. Upadhyay, M. Warner, W. Welfare, D.M. Livermore, N. Woodford, Emergence of a new antibiotic resistance mechanism in India, Pakistan, and the UK: a molecular, biological, and epidemiological study, Lancet Infect. Dis. 10 (2010) 597–602. https://doi.org/10.1016/S1473-3099(10)70143-2.

[11] P. Linciano, L. Cendron, E. Gianquinto, F. Spyrakis, D. Tondi, Ten years with New Delhi Metallo-β-lactamase-1 (NDM-1): from structural insights to inhibitor design, ACS Infect. Dis. 5 (2019) 9–34. https://doi.org/10.1021/acsinfecdis.8b00247.

[12] Venatorx Pharmaceuticals, Inc., A phase 3, randomized, double-blind, active controlled noninferiority study evaluating the efficacy, safety, and tolerability of cefepime/VNRX-5133 in adults with complicated urinary tract infections (cUTI), including acute pyelonephritis,

clinicaltrials.gov, 2021. https://clinicaltrials.gov/ct2/show/NCT03840148 (accessed August 31, 2021).
[13] M. Zalacain, C. Lozano, A. Llanos, N. Sprynski, T. Valmont, C. De Piano, D. Davies, S. Leiris, C. Sable, A. Ledoux, I. Morrissey, M. Lemonnier, M. Everett, Novel Specific Metallo-β-Lactamase Inhibitor ANT2681 Restores Meropenem Activity to Clinically Effective Levels against NDM-Positive *Enterobacterales*, Antimicrob. Agents Chemother. 65 (2021) e00203-21. https://doi.org/10.1128/AAC.00203-21.
[14] P.W. Groundwater, S. Xu, F. Lai, L. Váradi, J. Tan, J.D. Perry, D.E. Hibbs, New Delhi metallo-β-lactamase-1: structure, inhibitors and detection of producers, Future Med. Chem. 8 (2016) 993–1012. https://doi.org/10.4155/fmc-2016-0015.
[15] Y.-J. Zhang, X.-L. Liu, W.-M. Wang, C. Chen, M.-H. Zhao, K.-W. Yang, Amino acid thioesters exhibit inhibitory activity against B1–B3 subclasses of metallo-β-lactamases, Chem. Pharm. Bull. (Tokyo). 67 (2019) 135–142. https://doi.org/10.1248/cpb.c18-00717.
[16] Schrödinger Suite Schrödinger, LLC, New York, NY., 2011.
[17] ChemBioFrance - Infrastructure de recherche, (n.d.). https://chembiofrance.cn.cnrs.fr/en/composante/chimiotheque (accessed September 1, 2021).
[18] D.S. Wishart, Y.D. Feunang, A.C. Guo, E.J. Lo, A. Marcu, J.R. Grant, T. Sajed, D. Johnson, C. Li, Z. Sayeeda, N. Assempour, I. Iynkkaran, Y. Liu, A. Maciejewski, N. Gale, A. Wilson, L. Chin, R. Cummings, D. Le, A. Pon, C. Knox, M. Wilson, DrugBank 5.0: a major update to the DrugBank database for 2018, Nucleic Acids Res. 46 (2018) D1074–D1082. https://doi.org/10.1093/nar/gkx1037.
[19] T. Sterling, J.J. Irwin, ZINC 15 – Ligand discovery for everyone, J. Chem. Inf. Model. 55 (2015) 2324–2337. https://doi.org/10.1021/acs.jcim.5b00559.
[20] C.A. Lipinski, Rule of five in 2015 and beyond: Target and ligand structural limitations, ligand chemistry structure and drug discovery project decisions, Underst. Chall. -Rule--5 Compd. 101 (2016) 34–41. https://doi.org/10.1016/j.addr.2016.04.029.
[21] GOLD (Cambridge Crystallographic Data Center, CCDC, UK), n.d.
[22] G. Jones, P. Willett, R.C. Glen, A.R. Leach, R. Taylor, Development and validation of a genetic algorithm for flexible docking, J. Mol. Biol. 267 (1997) 727–748. https://doi.org/10.1006/jmbi.1996.0897.
[23] T. Sander, J. Freyss, M. von Korff, C. Rufener, DataWarrior: an open-source program for chemistry aware data visualization and analysis, J. Chem. Inf. Model. 55 (2015) 460–473. https://doi.org/10.1021/ci500588j.
[24] T. Liu, M. Naderi, C. Alvin, S. Mukhopadhyay, M. Brylinski, Break down in order to build up: decomposing small molecules for fragment-based drug design with eMolFrag, J. Chem. Inf. Model. 57 (2017) 627–631. https://doi.org/10.1021/acs.jcim.6b00596.
[25] J. Song, M. Mishima, Z. Rappoport, Isomeric solid enols on ring- and amide-carbonyls of substituted 2-carbanilido-1,3-indandiones, Org. Lett. 9 (2007) 4307–4310. https://doi.org/10.1021/ol7018554.
[26] Á.L. Fuentes de Arriba, E. Lenci, M. Sonawane, O. Formery, D.J. Dixon, Iridium-catalyzed reductive strecker reaction for late-stage amide and lactam cyanation, Angew. Chem. Int. Ed. 56 (2017) 3655–3659. https://doi.org/10.1002/anie.201612367.
[27] C.V. Credille, B.L. Dick, C.N. Morrison, R.W. Stokes, R.N. Adamek, N.C. Wu, I.A. Wilson, S.M. Cohen, Structure–Activity Relationships in Metal-Binding Pharmacophores for Influenza Endonuclease, J. Med. Chem. 61 (2018) 10206–10217. https://doi.org/10.1021/acs.jmedchem.8b01363.
[28] J.A. Day, S.M. Cohen, Investigating the Selectivity of Metalloenzyme Inhibitors, J. Med. Chem. 56 (2013) 7997–8007. https://doi.org/10.1021/jm401053m.

[29] Y. Guo, J. Wang, G. Niu, W. Shui, Y. Sun, H. Zhou, Y. Zhang, C. Yang, Z. Lou, Z. Rao, A structural view of the antibiotic degradation enzyme NDM-1 from a superbug, Protein Cell. 2 (2011) 384–394. https://doi.org/10.1007/s13238-011-1055-9.
[30] A. Proschak, G. Martinelli, D. Frank, M.J. Rotter, S. Brunst, L. Weizel, L.D. Burgers, R. Fürst, E. Proschak, I. Sosič, S. Gobec, T.A. Wichelhaus, Nitroxoline and its derivatives are potent inhibitors of metallo-β-lactamases, Eur. J. Med. Chem. 228 (2022) 113975. https://doi.org/10.1016/j.ejmech.2021.113975.
[31] P.K. Chrysanthopoulos, P. Mujumdar, L.A. Woods, O. Dolezal, B. Ren, T.S. Peat, S.-A. Poulsen, Identification of a New Zinc Binding Chemotype by Fragment Screening, J. Med. Chem. 60 (2017) 7333–7349. https://doi.org/10.1021/acs.jmedchem.7b00606.
[32] A.Y. Chen, P.W. Thomas, A.C. Stewart, A. Bergstrom, Z. Cheng, C. Miller, C.R. Bethel, S.H. Marshall, C.V. Credille, C.L. Riley, R.C. Page, R.A. Bonomo, M.W. Crowder, D.L. Tierney, W. Fast, S.M. Cohen, Dipicolinic Acid Derivatives as Inhibitors of New Delhi Metallo-β-lactamase-1, J. Med. Chem. 60 (2017) 7267–7283. https://doi.org/10.1021/acs.jmedchem.7b00407.
[33] M. Brindisi, S. Brogi, S. Giovani, S. Gemma, S. Lamponi, F. De Luca, E. Novellino, G. Campiani, J.-D. Docquier, S. Butini, Targeting clinically-relevant metallo- β-lactamases: from high-throughput docking to broad-spectrum inhibitors, J. Enzyme Inhib. Med. Chem. 31 (2016) 98–109. https://doi.org/10.3109/14756366.2016.1172575.
[34] S.B. Falconer, S.A. Reid-Yu, A.M. King, S.S. Gehrke, W. Wang, J.F. Britten, B.K. Coombes, G.D. Wright, E.D. Brown, Zinc Chelation by a Small-Molecule Adjuvant Potentiates Meropenem Activity in Vivo against NDM-1-Producing *Klebsiella pneumoniae*, ACS Infect. Dis. 1 (2015) 533–543. https://doi.org/10.1021/acsinfecdis.5b00033.
[35] Z. Muhammad, S. Skagseth, M. Boomgaren, S. Akhter, C. Fröhlich, A. Ismael, T. Christopeit, A. Bayer, H.-K.S. Leiros, Structural studies of triazole inhibitors with promising inhibitor effects against antibiotic resistance metallo-β-lactamases, Bioorg. Med. Chem. 28 (2020) 115598. https://doi.org/10.1016/j.bmc.2020.115598.
[36] G. Rivière, S. Oueslati, M. Gayral, J.-B. Créchet, N. Nhiri, E. Jacquet, J.-C. Cintrat, F. Giraud, C. van Heijenoort, E. Lescop, S. Pethe, B.I. Iorga, T. Naas, E. Guittet, N. Morellet, NMR Characterization of the Influence of Zinc(II) Ions on the Structural and Dynamic Behavior of the New Delhi Metallo-β-Lactamase-1 and on the Binding with Flavonols as Inhibitors, ACS Omega. 5 (2020) 10466–10480. https://doi.org/10.1021/acsomega.0c00590.
[37] K. Hanaya, M. Suetsugu, S. Saijo, I. Yamato, S. Aoki, Potent inhibition of dinuclear zinc(II) peptidase, an aminopeptidase from Aeromonas proteolytica, by 8-quinolinol derivatives: inhibitor design based on Zn2+ fluorophores, kinetic, and X-ray crystallographic study, JBIC J. Biol. Inorg. Chem. 17 (2012) 517–529. https://doi.org/10.1007/s00775-012-0873-4.
[38] E. Boukherrouba, C. Larosa, K.-A. Nguyen, J. Caburet, L. Lunven, H. Bonnet, A. Fortuné, A. Boumendjel, B. Boucherle, S. Chierici, M. Peuchmaur, Exploring the structure-activity relationship of benzylidene-2,3-dihydro-1H-inden-1-one compared to benzofuran-3(2H)-one derivatives as inhibitors of tau amyloid fibers, Eur. J. Med. Chem. 231 (2022) 114139. https://doi.org/10.1016/j.ejmech.2022.114139.
[39] A. Meguellati, A. Ahmed-Belkacem, W. Yi, R. Haudecoeur, M. Crouillère, R. Brillet, J.-M. Pawlotsky, A. Boumendjel, M. Peuchmaur, B-ring modified aurones as promising allosteric inhibitors of hepatitis C virus RNA-dependent RNA polymerase, Eur. J. Med. Chem. 80 (2014) 579–592. https://doi.org/10.1016/j.ejmech.2014.04.005.
[40] F. Zouhiri, J.-F. Mouscadet, K. Mekouar, D. Desmaële, D. Savouré, H. Leh, F. Subra, M. Le Bret, C. Auclair, J. d'Angelo, Structure−Activity Relationships and Binding Mode of Styrylquinolines as Potent Inhibitors of HIV-1 Integrase and Replication of HIV-1 in Cell Culture, J. Med. Chem. 43 (2000) 1533–1540. https://doi.org/10.1021/jm990467o.
[41] E. Harder, W. Damm, J. Maple, C. Wu, M. Reboul, J.Y. Xiang, L. Wang, D. Lupyan, M.K. Dahlgren, J.L. Knight, J.W. Kaus, D.S. Cerutti, G. Krilov, W.L. Jorgensen, R. Abel, R.A. Friesner,

OPLS3: a force field providing broad coverage of drug-like small molecules and proteins, J. Chem. Theory Comput. 12 (2016) 281–296. https://doi.org/10.1021/acs.jctc.5b00864.
[42] H. Zhang, G. Ma, Y. Zhu, L. Zeng, A. Ahmad, C. Wang, B. Pang, H. Fang, L. Zhao, Q. Hao, Active site conformational fluctuations promote the enzymatic activity of NDM-1, Antimicrob. Agents Chemother. (2018) AAC.01579-18. https://doi.org/10.1128/AAC.01579-18.
[43] M.D. Eldridge, C.W. Murray, T.R. Auton, G.V. Paolini, R.P. Mee, Empirical scoring functions: I. The development of a fast empirical scoring function to estimate the binding affinity of ligands in receptor complexes, J. Comput. Aided Mol. Des. 11 (1997) 425–445. https://doi.org/10.1023/A:1007996124545.
[44] M.J. Frisch, G.W. Trucks, H.B. Schlegel, G.E. Scuseria, M.A. Robb, J.R. Cheeseman, G. Scalmani, V. Barone, G.A. Petersson, H. Nakatsuji, X. Li, M. Caricato, A.V. Marenich, J. Bloino, B.G. Janesko, R. Gomperts, B. Mennucci, H.P. Hratchian, J.V. Ortiz, A.F. Izmaylov, J.L. Sonnenberg, Williams, F. Ding, F. Lipparini, F. Egidi, J. Goings, B. Peng, A. Petrone, T. Henderson, D. Ranasinghe, V.G. Zakrzewski, J. Gao, N. Rega, G. Zheng, W. Liang, M. Hada, M. Ehara, K. Toyota, R. Fukuda, J. Hasegawa, M. Ishida, T. Nakajima, Y. Honda, O. Kitao, H. Nakai, T. Vreven, K. Throssell, J.A. Montgomery Jr., J.E. Peralta, F. Ogliaro, M.J. Bearpark, J.J. Heyd, E.N. Brothers, K.N. Kudin, V.N. Staroverov, T.A. Keith, R. Kobayashi, J. Normand, K. Raghavachari, A.P. Rendell, J.C. Burant, S.S. Iyengar, J. Tomasi, M. Cossi, J.M. Millam, M. Klene, C. Adamo, R. Cammi, J.W. Ochterski, R.L. Martin, K. Morokuma, O. Farkas, J.B. Foresman, D.J. Fox, Gaussian 16 Rev. C.01, Wallingford, CT, 2016.
[45] H.S. Yu, X. He, S.L. Li, D.G. Truhlar, MN15: A Kohn–Sham global-hybrid exchange–correlation density functional with broad accuracy for multi-reference and single-reference systems and noncovalent interactions, Chem Sci. 7 (2016) 5032–5051. https://doi.org/10.1039/C6SC00705H.
[46] F. Weigend, Accurate Coulomb-fitting basis sets for H to Rn, Phys Chem Chem Phys. 8 (2006) 1057–1065. https://doi.org/10.1039/B515623H.
[47] F. Weigend, R. Ahlrichs, Balanced basis sets of split valence, triple zeta valence and quadruple zeta valence quality for H to Rn: Design and assessment of accuracy, Phys Chem Chem Phys. 7 (2005) 3297–3305. https://doi.org/10.1039/B508541A.
[48] J. Tomasi, B. Mennucci, R. Cammi, Quantum mechanical continuum solvation models, Chem. Rev. 105 (2005) 2999–3094. https://doi.org/10.1021/cr9904009.
[49] E. Tremey, F. Bonnot, Y. Moreau, C. Berthomieu, A. Desbois, V. Favaudon, G. Blondin, C. Houée-Levin, V. Nivière, Hydrogen bonding to the cysteine ligand of superoxide reductase: acid–base control of the reaction intermediates, JBIC J. Biol. Inorg. Chem. 18 (2013) 815–830. https://doi.org/10.1007/s00775-013-1025-1.
[50] Z. Nazarian, C. Forsyth, Double cyclization of O-acylated hydroxyamides generates 1,6-dioxa-3,9-diazaspiro[4.4]nonanes a new class of oxy-oxazolidinones, RSC Adv. 6 (2016) 55534–55538. https://doi.org/10.1039/C6RA11604C.
[51] C.J. Perry, Z. Parveen, The cyclisation of substituted phthalanilic acids in acetic acid solution. A kinetic study of substituted N-phenylphthalimide formation, J. Chem. Soc. Perkin Trans. 2. (2001) 512–521. https://doi.org/10.1039/b008399m.
[52] I. Mierina, A. Stikute, A. Mishnev, M. Jure, An alternative way to analogues of avenanthramides and their antiradical activity, Monatshefte Für Chem. - Chem. Mon. 150 (2019) 85–101. https://doi.org/10.1007/s00706-018-2288-6.
[53] E. Malamidou-Xenikaki, S. Spyroudis, M. Tsanakopoulou, Studies on the reactivity of aryliodonium ylides of 2-hydroxy-1,4-naphthoquinone: reactions with amines, J. Org. Chem. 68 (2003) 5627–5631. https://doi.org/10.1021/jo0343679.
[54] P.A. Wiget, L.A. Manzano, J.M. Pruet, G. Gao, R. Saito, A.F. Monzingo, K.R. Jasheway, J.D. Robertus, E.V. Anslyn, Sulfur incorporation generally improves Ricin inhibition in pterin-appended glycine-phenylalanine dipeptide mimics, Bioorg. Med. Chem. Lett. 23 (2013) 6799–6804. https://doi.org/10.1016/j.bmcl.2013.10.017.

[55] S. Hackbusch, A.H. Franz, Acylation of trans-2-substituted cyclohexanols: the impact of substituent variation on the pyridine-induced reversal of diastereoselectivity, Arkivoc. 2015 (2015) 172–194. https://doi.org/10.3998/ark.5550190.p009.321.
[56] H. Pessoa-Mahana, J. Kosche C., N. Ron H., G. Recabarren-Gajardo, C. Saitz B., R. Araya-Maturana, C. David Pessoa-Mahana, Solvent-free microwave synthesis of 3-(4-benzo[b]thiophene-2-carbonyl)-1-piperazinyl-1-benzo[b]thiophen-2-yl-1-propanones. New hetero bis-ligands with potential 5-HT1A serotonergic activity, Heterocycles. 75 (2008) 1913. https://doi.org/10.3987/COM-08-11326.
[57] M.K. Christensen, K.D. Erichsen, U.H. Olesen, J. Tjørnelund, P. Fristrup, A. Thougaard, S.J. Nielsen, M. Sehested, P.B. Jensen, E. Loza, I. Kalvinsh, A. Garten, W. Kiess, F. Björkling, Nicotinamide phosphoribosyltransferase inhibitors, design, preparation, and structure–activity relationship, J. Med. Chem. 56 (2013) 9071–9088. https://doi.org/10.1021/jm4009949.
[58] K. Mekouar, J.-F. Mouscadet, D. Desmaële, F. Subra, H. Leh, D. Savouré, C. Auclair, J. d'Angelo, Styrylquinoline Derivatives: A New Class of Potent HIV-1 Integrase Inhibitors That Block HIV-1 Replication in CEM Cells, J. Med. Chem. 41 (1998) 2846–2857. https://doi.org/10.1021/jm980043e.
[59] G. Delapierre, J.M. Brunel, T. Constantieux, G. Buono, Design of a new class of chiral quinoline–phosphine ligands. Synthesis and application in asymmetric catalysis, Tetrahedron Asymmetry. 12 (2001) 1345–1352. https://doi.org/10.1016/S0957-4166(01)00220-8.
[60] A. Legru, F. Verdirosa, J.-F. Hernandez, G. Tassone, F. Sannio, M. Benvenuti, P.-A. Conde, G. Bossis, C.A. Thomas, M.W. Crowder, M. Dillenberger, K. Becker, C. Pozzi, S. Mangani, J.-D. Docquier, L. Gavara, 1,2,4-Triazole-3-thione compounds with a 4-ethyl alkyl/aryl sulfide substituent are broad-spectrum metallo-β-lactamase inhibitors with re-sensitization activity, Eur. J. Med. Chem. 226 (2021) 113873. https://doi.org/10.1016/j.ejmech.2021.113873.
[61] M.J. Martin, B.W. Corey, F. Sannio, L.R. Hall, U. MacDonald, B.T. Jones, E.G. Mills, C. Harless, J. Stam, R. Maybank, Y. Kwak, K. Schaufler, K. Becker, N.-O. Hübner, S. Cresti, G. Tordini, M. Valassina, M.G. Cusi, J.W. Bennett, T.A. Russo, P.T. McGann, F. Lebreton, J.-D. Docquier, Anatomy of an extensively drug-resistant *Klebsiella pneumoniae* outbreak in Tuscany, Italy, Proc. Natl. Acad. Sci. 118 (2021) e2110227118. https://doi.org/10.1073/pnas.2110227118.
[62] Clinical and Laboratory Standards Institute (CLSI). 2015. M07-A10: Methods for Dilution Antimicrobial Susceptibility Tests for Bacteria That Grow Aerobically; Approved Standard - Tenth Edition., (n.d.).